

1-1-1979

# Study of the reticular floor slab system.

Clarence Au-Young

Follow this and additional works at: <http://preserve.lehigh.edu/etd>



Part of the [Civil Engineering Commons](#)

---

## Recommended Citation

Au-Young, Clarence, "Study of the reticular floor slab system." (1979). *Theses and Dissertations*. Paper 1868.

This Thesis is brought to you for free and open access by Lehigh Preserve. It has been accepted for inclusion in Theses and Dissertations by an authorized administrator of Lehigh Preserve. For more information, please contact [preserve@lehigh.edu](mailto:preserve@lehigh.edu).

STUDY OF THE RETICULAR FLOOR  
SLAB SYSTEM

by  
Clarence Au-Young

A THESIS  
Presented to the Graduate Committee  
of Lehigh University  
in Candidacy for the Degree of  
Master of Science  
in  
Civil Engineering

Lehigh University

1979

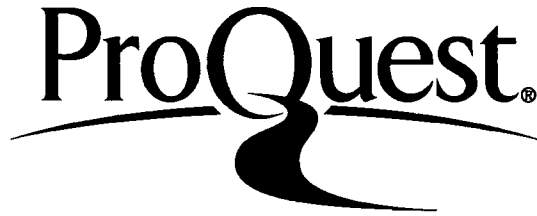
ProQuest Number: EP76140

All rights reserved

INFORMATION TO ALL USERS

The quality of this reproduction is dependent upon the quality of the copy submitted.

In the unlikely event that the author did not send a complete manuscript and there are missing pages, these will be noted. Also, if material had to be removed, a note will indicate the deletion.



ProQuest EP76140

Published by ProQuest LLC (2015). Copyright of the Dissertation is held by the Author.

All rights reserved.

This work is protected against unauthorized copying under Title 17, United States Code  
Microform Edition © ProQuest LLC.

ProQuest LLC.  
789 East Eisenhower Parkway  
P.O. Box 1346  
Ann Arbor, MI 48106 - 1346

This thesis is accepted and approved in partial fulfillment of the requirements for the degree of Master of Science in Civil Engineering.

June 8, 1979  
Date

\_\_\_\_\_  
Professor in Charge

\_\_\_\_\_  
Chairman of Department

## ACKNOWLEDGMENTS

This study was carried out under the direct supervision of Dr. Ti Huang and Dr. Le Wu Lu. Their valuable suggestions and guidance throughout the study is gratefully acknowledged. Special thanks are also due to M. Nakashima who participated in most experimental tests. Also, H. T. Sutherland, Instruments Associate and the Fritz Engineering Laboratory support staff under the supervision of R. R. Dales; K. Eberts, and R. Hittenger, provided assistance throughout the laboratory work.

Thanks are also due to Kathryn Skaar for her preparation of the manuscript and to R. Sopko for the photographic coverage.

## TABLE OF CONTENTS

	<u>Page</u>
Abstract	1.
1. INTRODUCTION	2.
1.1 Background	2.
1.2 Objectives	4.
1.3 Scope	5.
2. EXPERIMENTAL WORK	6.
2.1 Concrete Mix	6.
2.2 Filler Boxes	7.
2.3 Reinforcement	8.
2.4 Testing of Joist Specimen	8.
2.5 Strip Specimen	9.
2.6 Slab Model	11.
3. EXPERIMENTAL RESULTS	17.
3.1 Joist Specimen	17.
3.2 Strip Specimen	17.
3.3 Slab Specimen	18.
4. DATA ANALYSIS AND THEORETICAL STUDY USING FINITE ELEMENT MODEL	20.
4.1 Preparation of Finite Element Model	20.
4.2 Discretization of Finite Element Model	21.
4.3 Simulated Load Test	22.
4.4 Parametric Study Using Finite Element Models	23.
5. CONCLUSION AND REMARKS	27.
6. TABLES	30.

	<u>Page</u>
7. FIGURES	34.
8. BIBLIOGRAPHY	67.
9. VITA	68.

## LIST OF TABLES

	<u>Page</u>
1. Mix of filler boxes for 1 m <sup>3</sup> of concrete	31.
2. Gradation of sand for filler box mix	31.
3. Mix of joists and slab for 1 m <sup>3</sup> of concrete	31.
4. Gradation of sand for the slab specimen	32.
5. Properties of steel reinforcements	32.
6. Elastic load tests performed on slab specimen	33.
7. Stiffness characteristics of slab specimen determined from elastic tests	33.



## LIST OF FIGURES

	<u>Page</u>
1. Typical Example Of A Column Grid System	35.
2. Isometric View And Dimensions Of A Filler Box	36.
3. Plexiglass Mold For Filler Boxes	36.
4. Dimension And Cross-Sectional Detail Of The Joist Specimen	37.
5. Dimension And Cross-Sectional Detail of the Strip Specimen	37.
6. Schematic Setup For The Strip Specimen	38.
7. Test Setup For The Strip Specimen	38.
8. Additional Reinforcement In Solid Corner Panel	39.
9. Vertical Stirrups For The Outer Joists	39.
10. Design Detail Of The Slab Specimen	40.
11. Formwork For Slab Specimen Before Casting	41.
12. Schematic Setup For Moment Application	41.
13. Elastic Test Setup For The Slab Model	42.
14. Location Of Dial Gages For Elastic Tests	42.
15. Dial Gages Setup For Elastic Tests	43.
16. Rotation Gages Used For Slab Test	43.
17. Location Of Dial Gages For The Ultimate Load Test	44.
18. Instrument Setup In The Ultimate Load Test	45.
19. First Layer Of Loading Device On The Slab Model	45.
20. Second Layer Of Loading Device	46.
21. Final Layer Of Loading Device	46.
22. Complete Loading Setup For The Ultimate Test Of The Slab Specimen	47.

	<u>Page</u>
23. One Loading Corner Broke Off From The Slab Model At An Applied Moment of 444.4 N-M	47.
24. Similar Failure Occurred At The Other Corner At 533.3 N-M	48.
25. Load-Deflection Curve For Mid-Span Of Joist Specimen	49.
26. Joist Specimen After Ultimate Failure	50.
27. Mid-Span Crack Of Strip Specimen Before Ultimate Failure	50.
28. Load-Deflection Curve For Mid-Span Of The First Strip Specimen	51.
29. Load-Deflection Curve For Mid-Span Of The Second Strip Specimen	52.
30. Average Rotation At Loaded Corners For Test 1	53.
31. Average Rotation At Loaded Corners For Test 2	54.
32. Rotation At The Loaded Corner For Test 3	55.
33. Average Rotation At The Loaded Corners For Test 4	56.
34. Slab Specimen At Completion Of All Load Tests	57.
35. Comparison Between Experimental Test Results And Theoretical Analysis For Joist Specimen	58.
36. Comparison Between Experimental Results Of Strip Specimen And A Fictitious I-Beam With Flange Width Of 56 mm	59.
37. Discretization Of Finite Element Model	60.
38. Comparison Between Experimental Results Of Slab Model And Finite Element Analysis For Test 4	61.
39. Comparison Between Test Results And Finite Element Analysis For Test 1	62.
40. Comparison Between Test Results And Finite Element Analysis For Test 2	63.

	<u>Page</u>
41. Comparison Between Test Results And Finite Element Analysis For Test 3	64.
42. Parma's Model In Determining Coefficient Of Torsional Efficiency	65.
43. Torsional Coefficient Curves For Various Slab Models	66.

## ABSTRACT

A floor slab system composed of precast concrete hollow boxes and reinforced cast-in-place joists has been widely adopted in several Latin American countries for the past two decades. This floor slab, called the reticular system, poses certain advantages over the conventional concrete floor system being used in the United States. This project is a continuation of a joint project between Lehigh University and the Escuela Colombiana de Ingenieria in Colombia to investigate the characteristics of the system of which little is known up to now. Test models included a single reinforced joist, two strip specimens, each of which consisted of two parallel reinforced joists cast with a row of six hollow boxes in between; and a six box square slab specimen. While only vertical load tests were performed on the first two types of models, the slab specimen was subjected to both vertical service loads and applied corner moments which simulated the effect of lateral load. Finite element analyses of these results showed that the precast box acts compositely with the joists, giving an effective flange width of 22% of the total width of the box on each side of the reinforced joists. The torsional efficiency coefficient of the studied specimen as a function of aspect ratio has been obtained from a computer analysis and it is shown that such a relationship can be used in the design of the reticular system.

## 1. INTRODUCTION

### 1.1 Background

A concrete floor system similar to waffle slab has been growing increasingly popular in several Latin American countries such as Colombia, Venezuela and Ecuador. Since it was first introduced in 1949 by Domenico Parma of Bogota, Colombia, millions of square meters of this slab system has been constructed in that country. The system, known as the reticular system, consists of precast concrete hollow boxes and reinforced cast-in-place concrete joists which intersected at right angles as shown in Fig. 1. This system resembles waffle slab in the sense that they both utilize a grid of joists as the primary load carrying elements. Both are thinner in total depth than other floor systems and result in smaller story heights. Moreover, no supporting beams or column capitals are necessary below the slab. The reticular system, however, offers further advantages over the conventional waffle slab. Except at locations where heavy concentrated loads are applied, such as in parking garages, cast-in-place top slab is not required. This system gives an overall smooth surface that is not offered by other systems.

With the above described advantages, the reticular system seems to be well suited for multi-story building structures. Unfortunately, very little research has been carried out to study the structural behavior of this slab system, particularly with regard to seismic loading. It appeared that Parma (Ref. 1) hitherto was the only one who

had investigated more extensively into such a system and developed some form of design guidelines. At present, design of such slab structure still involves many uncertainties and many designers are reluctant to use this floor system.

In recent years, it was viewed that since a large part of the United States is subjected to earthquake of a severity similar to that in Colombia, and since this grid system has been shown to be effective in Colombia by more than two decades existence, its use in the United States is worth exploring. Before any acceptable design specification could be drawn up, however, careful research must be conducted so that the characteristics of such system would be sufficiently understood. For this purpose, a joint research study by Lehigh University and the Escuela Colombiana de Ingenieria, Colombia, was conducted. At Lehigh University, the work was divided into two phases. The first, which was completed by Armando Palamino (Ref. 2) in late 1977, focused on the behavior of the floor slab under gravity load only. The second phase, which constitutes the theme of this report, deals with the response of such system to lateral load.

## 1.2 Objectives

The objectives of this phase of the study are threefold:

1. To establish from experimental test data an acceptable simulation model of the slab that could be analyzed by the finite element method.
2. To perform parametric study of the floor system using the finite element method.
3. To develop design curves for this slab system and to suggest needed further research.

### 1.3 Scope

Tests were conducted on progressively larger components of this system. Reinforced concrete joists were first tested to establish their sectional properties. Two strips, each consisting of a series of six box panels cast in between two joists, were then subjected to bending test. The data so obtained were compared with those from the joist test, and the width of the box sections that participated in resisting bending moments were determined. Finally, a square slab model with six boxes in each direction was then subjected to corner moments which simulated the effects of forces. Several tests of this type were performed within the elastic range, using different support and loading arrangements. Deflections as well as rotations were measured at several selected locations. The specimen was then loaded with vertical design service load combined with equal bending moments increasingly applied at all four simple supported corners in an attempt to bring it to ultimate failure.

Using the effective sectional properties determined from the strip and joist tests, a finite element model of the slab specimen was developed and was analyzed with the use of SAP IV programs, under the same loading condition as used in the slab test. The results were then compared with those from the experimental tests.



## 2. EXPERIMENTAL WORK

### 2.1 Concrete Mix

Different concrete mixes were used for the filling boxes and the joists. In addition, the mixes for the reinforced joists were changed slightly as the project went along.

The mix for the filler boxes is shown in Table 1, and the sand gradation is shown in Table 2. Type I Portland cement was used. Very small aggregates were used for the mix because of the small dimensions of the specimen (see section 2.6), and to be comparable with the micro-concrete used by the Colombian research group.

Concrete mix for the joists of all the specimens is shown in Table 3 and the sand gradation of the mix is shown in Table 4. All joist and strip specimens prepared from the above mix were found to contain a large number of voids. As a result, in addition to the basic mix, 0.0018 m<sup>3</sup> of water reducing agent for each cubic meter of concrete was used for the slab specimen. The concrete thus obtained was found to be more workable. The water cement ratio for all concrete was 0.60 by weight.

At different stages of the research, cylinder tests were performed for the various concrete used. Concrete from filler boxes were all 1" x 2" cylinders while samples of all other mixes were 3" x 6" cylinders. The uncorrected average compressive strengths are as follows:

Beam and strip specimen	9.64 MPa
Slab specimen	9.70 MPa
Filler boxes	11.02 MPa

Except for that of the filler boxes, all figures above were 28 day

strengths. The higher strength possessed by the slab concrete was due to the improved mix with the added water reducing agent.

Due to the long process of fabrication required, the filler boxes had varying ages from three months to two years at the time of the casting of the slab specimen. In order to avoid too wide a variation in strength, all boxes used in the slab model were chosen to be the most recent ones and their ages differed by no more than nine months. The average strength determined for all boxes used in the slab model was 10.37 MPa.

## 2.2 Filler Boxes

The filler boxes were fabricated in halves, each having the dimensions 179 x 179 x 36 mm, as shown in Fig. 2. The wall thickness varied linearly from 4 mm at the open edge to 5 mm at the connection with the base plate which was 6 mm thick. The dimensions of the specimens were obtained by a one-fifth reduction from a prototype 900 x 900 x 180 mm. During casting, two of these pans were placed face to face, creating a hollow box. Obviously, the thickness of the finished slab was actually twice the height of these precast boxes, or 72 mm for the model.

All boxes were cast in plexiglass molds shown in Fig. 3. The formwork was stripped off after three days of curing in the steamroom. Due to the delicate nature of the boxes, casting and demolding had to be done very carefully. A specific procedure was followed in order to avoid excessive tapping or pulling forces being exerted on the boxes. Even with all the precautions, the success rate was as low as three to

four pans out of a batch of six. After demolding, the good boxes were cured in a curing room until cast into test specimens.

### 2.3 Reinforcement

Since deformed steel wires of suitable sizes are not commercially available in the United States, special reinforcement was shipped in from Colombia. Deformations were made onto the surface of these reinforcing wires by a specially designed tool. Afterwards, these wires were annealed in an electric oven to achieve the desirable yield stress. The average yield point stress of the wires after deformation and annealing was 293 MPa.

Wires of four different sizes were used in the original design. The diameters were 3.4 mm, 2.75 mm, 2.0 mm and 1.27 mm respectively. All wires were used as longitudinal reinforcements except for the smallest one which was also used for stirrups.

Stirrups in the slab specimen were also fabricated out of smooth wires manufactured in the United States. This was necessitated by the exhaustion of the Colombian wires stored at Fritz Engineering Laboratory. These United States wires had a smaller diameter of only 0.74 mm, but a much higher yield stress of 516 MPa. Table 5 shows the geometrical and mechanical properties of the reinforcements.

### 2.4 Teating of Joist Specimen

Only one joist was cast and tested. Its dimension and cross-sectional details are shown in Fig. 4. Except for the lack of vertical stirrups, all reinforcements were identical to that of the outermost joist of the slab specimen (VI in Fig. 10). The main objective of this

part of the tests was to compare the experimental results with, and consequently verify, results from theoretical analysis.

The joist was tested over a simple span of 980 mm with a pair of symmetrical concentrated loads located at 300 mm from each support. Vertical deflections were measured at mid-span and each of the 1/4 span mark by using dial gages sensitive to 0.025 mm (0.00/in.). The load was applied at increments of 133.3 N (30 lbs.) until ultimate failure occurred. The results of this test will be given in Section 3.1.

## 2.5 Strip Specimen

A strip specimen consisted of two parallel reinforced joists combined with a row of six boxes between them, as shown in Fig. 5. Two strip specimens with different joist reinforcements were tested. Both tests were conducted twenty-nine days after casting.

The first specimen had its joists reinforced exactly identical to the single joist specimen described in Section 2.4. Again, no shear reinforcement was provided. Some working problems were encountered during casting of the strip specimen. The filler boxes had a tendency to float and move around while concrete was being placed into the formworks. They were eventually held down by a steel angle that was fixed across the top of formwork. In addition, it was found that a model of such small size provided very little room to work. This problem was even more important in the preparation of the second specimen where the joists contained heavier reinforcement. Under the crowded condition, the 7 mm concrete cover required over the reinforcing wires was extremely

difficult to maintain throughout the length of the specimens. The problem was further complicated because most of the reinforcing wires were not straight to begin with. As a result, insufficient cover occurred at some locations.

Testing of the strip specimens were done under simulated uniformly distributed load. A specially designed loading setup was used to achieve this purpose. The setup consisted of a steel channel and ten pieces of plywood blocks of appropriate sizes, arranged with steel balls between them. This system of lever distributed a single concentrated load at the mid-span location into equal forces at twelve contact points on the specimen. This setup is illustrated in Fig. 6. Dial gages were installed at mid-span as well as each of the 1/4 span locations to measure vertical deflections. The specimen was tested over a simple span of 1200 mm. The entire test setup is shown in Fig. 7.

The single applied load was increased at initial increments of 222.2 N (50 lbs.) until cracks were detected, it was then increased at a smaller and varied increment until the specimen failed. At the point when ultimate failure was imminent, all dial gages were removed to prevent damages done to the instruments.

The second specimen was identical to the first one except for the bottom reinforcements in the joists. Three wires were used in each joist, 2.75 mm, 2.0 mm, and 1.27 mm respectively, giving a total area of  $10.35 \text{ mm}^2$ . The reinforcement is identical to that in joist V-2 in Fig. 10. When the formwork was stripped off, a week after casting, considerable honeycombing was found on the joists. This was probably due to the inadequate compaction of the concrete in view of the limited spacing in

in the formwork. These honeycomb spaces were eventually patched up before testing using concrete of the same mix. To avoid this problem from further occurrence, small quantities of water reducing agent was added to the mix for the slab model to increase the workability of the concrete.

Test setup and procedures for the second strip specimen was identical to that of the first strip.

## 2.6 Slab Model

The slab specimen tested was a 1221 mm square panel with a thickness of 72 mm (Fig. 8). Sixty-four filler boxes were used at thirty-two locations on the specimens. The four locations at the corners were cast into solid sections as practised in actual construction. Additional vertical stirrups as well as top reinforcements were also placed in the corners. This was done in order to strengthen the connections to columns at such corners. Shear reinforcements were also provided for the two outer joists close to each end. (Fig. 9)

All joists had top reinforcements with a steel area of  $3.14 \text{ mm}^2$ . Bottom reinforcement varied depending on the location of the joist. The design details and the formwork before casting are shown in Figs. 10 and 11, respectively. Except for slight differences in reinforcements and corner attachments, the slab specimen was identical to the one tested by Palomino (Ref. 2) using vertical load.

To facilitate attaching, loading and supporting apparatus, each of the four corners of the slab panel was enlarged by a 101.6 mm (4 in.) square corner piece, as is shown in Fig. 10. The theoretical corner,

at the intersection of the centerlines of joists V-1, was marked by an embedded steel tube with a 11.11 mm (7/16 in.) diameter. A steel plate 6.35 mm ( $\frac{1}{4}$  in.) thick was cast at the bottom of each corner piece, and the top reinforcing wires of the V-1 joists were extended into these pieces. No other reinforcement was used.

Specially fabricated steel bars were used as loading arms. Two holes were drilled in these bars so that they could be rigidly attached to the loading comers. The two connecting bolts, anchored in the concrete, were located symmetrically about the theoretical comer of the slab. Two small notches, exactly 1 m apart, were cut antisymmetrically on each loading arm. Through such device, a pair of equal and opposite force can be applied at the two notches to deliver a resultant corner moment to the specimen (Fig. 12).

In order to ensure solid compaction during casting, an electric vibrator acting on one side of the formwork was used in addition to the shaking table. Together with an improved mix, a very satisfactory casting was attained. The specimen was cured thirty-five days before testing.

Load tests of the slab were divided into two phases. The first phase was designed to establish some elastic characteristics of the slab under applied end moments. The second phase was an ultimate load test through which the specimen failed under increasing end moments applied equally at all four corners, while a vertical uniformly distributed load was maintained on the slab at the design service level. A loading frame was designed especially for the application of moments. When

hung above the specimen, the frame projected precisely on the loading arms so that pulleys could be inserted into them. For loading purpose, baskets of steel wire grids were made. Two baskets were used for each loading arm, one hanging directly at the upward notch while the other was hung on a pulley by a rope that pulled up at the other notch. By placing equal weights in the baskets, a moment equal to the product of the weights in one basket and the distance between the two notches would be created. This entire setup is shown in Fig. 13.

The testing of the slab specimen was done in the space under the five million pound Baldwin testing machine, with the loading frame attached to the machine's moving head. The use of the machine as the reacting bulkhead offered two distinct advantages. The vertical location of the moving head can be easily adjusted to suit the loading mechanisms. In addition, the machine was sensitive enough as a load measuring device so that load cells were not needed.

The specimen was supported by two parallel steel I-beams which in turn rested on the pedestal of the testing machine. The I-beams and the over 7000 Kg. pedestal were massive enough to create a rigid support condition to the test specimen.

For the first phase of the test, six dial gages were used. The gages were lined up under the center line of the third row of boxes, each one measuring the deflection at the center point of the box as illustrated in Figs. 14 and 15. Rotation gages were mounted on the appropriate loading arms where the rotations at those corners were to be measured. The rotation gage (Fig. 16) consisted of a dial gage



attached to a good piece that was supported on two ends, one of which could be adjusted vertically in order to keep the gage level.

Five elastic tests were conducted on the slab. The same tests were repeated with all the applied moments reversed. This was done to eliminate errors caused by instrumental inaccuracies. The test configurations are listed in their order in Table 6.

In order to stay safely within the elastic range, only six to seven moment increments of 44.4 N-M (10 lbs. x 1 m.) were applied in each test. Upward forces were applied in some tests to visibly lift the specimen off the supporting beam so that a pure cantilever action was ensured. Fixed end conditions were achieved by using two large C-clamps to fasten the protruding corners tightly to the flange of the supporting I-beam.

In Test 4, where moments were applied to two corners while the specimen rested on simple supports, rotations were induced on all four corners. In order to obtain more data on the stiffness of the slab, an attempt was made to determine the "carry-over" factor directly by applying moments to the "unloaded" corners, until the rotations at those corners were reduced to zero. However, since the metal weights used in the loading had fixed weights, it was highly improbable that the weights applied would just balance out the rotations. To overcome this problem, a series of different moments were applied at the corners and the corresponding rotations were measured. From the data thus obtained, a load-rotation curve was drawn. The moment required to balance the rotation could then be calculated by interpolation.

Determining the rotations of the corner by measuring the rotation of the attached loading arm created a problem, since the deformation of the loading arm must be taken into account. A calibration test was done to determine the rotation readings due to the deformation of the loading arm caused by applied moments. These were later deducted from the rotation readings measured during the slab test to give the net rotations of the slab corners.

In the second phase of the slab test, the specimen was simply supported at all corners. This condition was achieved by providing steel balls at the theoretical corner locations. Twelve dial gages were placed under the specimen to measure the vertical deflections at locations shown in Fig. 17. In addition, rotations in the direction of applied moments at the supports were measured by rotation gages with dials sensitive to 0.0025 mm (0.0001 in.).

In the first stage of the ultimate test, vertical load was first applied slowly to the specimen until a service load of approximately 3875 N/m (81 lbs./ft.<sup>2</sup>) was reached. The application of the vertical load was through a 13300 N (3000 lbs.) mechanical jack which acted against the movable machine head. This applied load was measured directly by the testing machine. A system of simply supported wooden blocks and steel beams was used to distribute the applied load to thirty-six equal components, each acting at the center of one filler box, as shown in Fig. 19, which was actually taken during Palomino's slab test. Since the same loading blocks were used in this slab test, the previously taken picture served well as an illustration of the loading system. Two more layers of wooden blocks were included in the

system, each placed in such a way so that the applied load was equally distributed to the layer underneath. These are shown in Figs. 20 and 21 in their order. The loading blocks were then topped by two identical I-beams placed symmetrically for equal load distribution. A final top I-beam completed the loading system. The entire setup is shown in Fig. 22.

The jack load was applied at increments of 444.4 N (100 lbs.) which was equivalent to incremental distributed loads of  $298.1 \text{ N/m}^2$  (81 lbs./ft.<sup>2</sup>). With the vertical load maintained at that level, corner moments in increments of 44.4 N-m were applied equally to all four corners. All moments were applied in the same direction simulating the effect of lateral sway. Both rotation and vertical deflection readings were recorded after each increment of load. During the course of the test, all cracks detected were marked at each load level and their propagation was closely watched. When corner moment reached 444.4 N-m (100 lbs. x 1 m.), one of the slab corners failed (Fig. 23) in a brittle manner. Additional loading was then applied to the corner which was symmetric to the failed corner, while moments at all other corners were kept constant at the 444.4 N-m. The load increment was substantially reduced since a similar failure at the loaded corner was expected to be imminent. Failure of this corner occurred when the applied moment reached 533.3 N-m (120 lbs. x 1 m.) (Fig. 24). The testing was then terminated without developing general failure in the slab.

### 3. EXPERIMENTAL RESULTS

#### 3.1 Joist Specimen

Figure 25 shows the relationship between applied load and mid-span deflection of the joist specimen. The first crack was detected at a load of 889 N (200 lbs.) at a section approximately 30 mm off the mid-span. This coincided well with the sudden deviation of the curve from its initial tangent. More cracks were detected at higher loads, all of them located within the constant moment region. Failure occurred at a load of 1222 N across the section where crack was first detected.

The specimen after failure is shown in Fig. 26.

#### 3.2 Strip Specimen

During the test of strip specimen 1, an initial crack was detected at a quarter span section under an applied load of 1400 N. The formation of this minute crack was coupled with a sudden deflection, possibly due to a movement of the support. More cracks developed as increasing load was applied. At a load of 2111 N, a major crack developed at mid-span. Its width grew rapidly from an initial base width of 0.8 mm to 3 mm at a load of 2355 N when it penetrated almost all the way to the top (Fig. 27), and the specimen started to unload. It was observed that the cracks were developed nearly symmetrically about the mid-section and none were found to cut across any filling box. A close examination of the failed specimen showed no visible separation between the boxes and the connecting joists. A crushing failure was detected at one support. This failure apparently was initiated at a load of 1400 N when a sudden deflection occurred. The load deflection curve up to

ultimate of Specimen 1 is shown in Fig. 28.

Specimen 2 behaved similarly to the previous specimen. A mid-span crack, which eventually caused failure, was initially developed at a load of 1111 N. Visible cracks were also formed at each quarter span section. The ultimate load reached was 2333 N. This was slightly higher than expected since the reduction in reinforcement in this specimen was anticipated to reduce the strength by more than a mere 0.9%. The load deflection curve for this specimen is given in Fig. 29.

At the conclusion of the test, a crack was again found across one of the supports. It was due to such findings in both strip tests that the decision was made to use an improved mix for the slab model.

### 3.3 Slab Specimen

For each elastic test listed in Table 4, a curve of applied moment versus rotation at the loaded corner was plotted. These curves were shown in their order in Figs. 30 through 33. Three of the curves shown were obtained by averaging the results from two identical tests with moments applied in opposite directions, which should eliminate most instrumental inaccuracies. This was not done in Test 2 because a sudden rigid movement at a fixed support during the course of one test caused a discontinuity in the displacement curve obtained. As a result, that particular set of test results were discarded and Fig. 29 was solely the result of one test. Table 7 gives the stiffness characteristics of the slab as determined from each test.

During the four sets of elastic tests, a few minute cracks on the top surface of the specimen around the loaded corners were detected.

Since the applied loads were safely below the anticipated cracking load, these cracks could not be caused by the loading. They were most probably due to shrinkage effects and were simply opened up under the applied load.

During the application of vertical distributed load in the ultimate load test, a crack at mid-section was detected at an applied vertical load of 4528 N (3037 N/m<sup>2</sup>). More cracks were developed as the load was increased to the service load level of 5777 N. At this stage, the crack at the mid-section had penetrated 45 mm into the slab and most other cracks had penetrated at least 30 mm. None of the cracks had a base width of more than 1.5 mm.

During the second stage of the ultimate test in which end moments were applied equally at all four corners while the vertical load was held constant at the service load level, no visible abrupt change was detected until applied moments of 355.5 N-m (80 lbs. x 1 m.) were reached. At that load point, an inclined crack suddenly opened up at one of the high stress corners. A noticeable amount of detached concrete powder was also found on the supporting I-beam. When the end moments were increased to 444.4 N-m (100 lbs. x 1 m.), ultimate failure occurred across the described crack and the corner block was completely broken off from the specimen. A collapse would have occurred if not for the reinforcing wire that was imbedded into both sides.

Sudden failure identical to that observed previously eventually occurred at the symmetric corner at a moment of 533.3 N-m and brought an end to the test. The specimen, after the completion of all the load tests, is shown in Fig. 34.

#### 4. DATA ANALYSIS AND THEORETICAL STUDY USING FINITE ELEMENT METHOD

##### 4.1 Preparation of Finite Element Model

In order to obtain reliable results from finite element analysis, the model must simulate closely the characteristics of the actual specimen. This was achieved by matching the testing results of the several components.

At first, the load-deflection curve from the joist test was compared to that from a theoretical analysis of a lending member having a flexural stiffness equal to  $EI$  of  $76700 \text{ N-m}^2$ . It is seen that the calculated stiffness agrees with the test curve very well. In fact, at no point did they differ by more than 5%. From this comparison, it was concluded that the joist behaved as well as anticipated and the properties of concrete obtained from cylinder tests were also within tolerance. Thus, for the finite element analysis, all actual joists present could be modelled by a three-dimensional beam of known elastic properties, provided that the analysis was within the elastic range.

Results from previous research studies (Ref. 2) indicated that the filler box sections were not fully effective in resisting bending, and it was the intention of this study to determine the portion of the boxes that contributed to load resistnace. This was done by utilizing the test results from the two strip specimens. Each strip was simulated by a fictitious flanged section where the web thickness equals the sum of the side joists of the strip together with the box walls and the flange width was made just wide enough to give the member the same stiff-

ness as the real strip. The flange width so obtained for both test strips agreed well with each other and averaged to be 56 mm or 31% of the box width. The comparison between a tested strip and its equivalent I-beam is shown in Fig. 3b. This same width was used in the finite element model for the slab specimen.

#### 4.2 Discretization of Finite Element Model

Discretization as shown in Fig. 37, was done in conformity with the format of SAP IV Program (Ref. 3). The slab was treated as a two-way grid where the joists were represented by beam elements with identical properties. In order that comparisons of deflections could be made between the computer result and the experimental data, the nodal points for the beam elements was located at the center of the filler boxes where the dial gages were placed during the slab test. The effect of the filler boxes was reflected in two respects. First, the torsional stiffness of the grid beams was computed for the full closed box section together with half a joist on each side. Secondly, for the bending stiffness of the grid beams, an effective flange width less than the full box width was used. The walls of the boxes were treated as an integral part of the reinforced joists, with the thickness adjusted according to the difference in Modulus of Elasticity. The initial trial flange width was 56 mm obtained by the strip analysis. This figure was obtained for pure bending situation and was not expected to be valid for the grid element which was subjected to combined torsion and bending. However, it did provide a starting value for the trial-and-error process by which the true width could be determined.



The scheme of having all six rows of boxes in each direction represented by the beam elements described above left the exterior half of all the edge joist unaccounted for and additional beam elements had to be instituted to complete the model. While the protruding loading blocks were represented by plate elements, the solid panel at each corner was treated as a beam element of appropriate properties in an effort to better reflect the heavy reinforcements in that area. The use of plate elements would have the disadvantage of not being able to bring out accurately the additional wiring used for both flexure and shear resistnace. All material property inputs were arrived at from actual weighing and cylinder tests.

#### 4.3 Simulated Load Test

As SAP IV analysis was only applicable to linear systems, all computer results were only applicable for elastic tests. A computer analysis on the ultimate load test would have to employ a more complicated program including non-linear and cracking responses. However, since a successful simulation on the elastic test would fulfill most of the objectives in this study, the use of a more complete program, such as NONSAP, was considered unnecessary.

The main purpose of the finite element tests was to determine the effective width of the box panels acting as the flange in the equivalent beams of the slab model. It was decided to select one of the four sets of elastic tests for initial comparison. When a satisfactory value was obtained, the other tests would then be used as verifications of the results thus determined. Test 4 (see Table 6) in which the slab was

simply supported at all four corners and with equal moments applied at two ends was chosen for this trial-and-error process.

An initial trial flange width of 56 mm was found to give deflections that were considerably smaller than the experimental test results. This reasonably implied that under combined action of flexure and torsion, the effective box width was smaller than if the specimen was subjected to bending alone. Decreasing values were subsequently tried and a satisfactory comparison, shown in Fig. 38, was obtained with a flange width of 0.044 m or 25% of this box width. Using the same effective width, computer load tests were then run for the remaining three sets of elastic tests and the results are shown in Figs. 39 to 41. Except for Test 3, the comparisons were within tolerance and were especially good for Test 1. The less than adequate comparison for Test 3 could be explained by the fact that an unsymmetrical loading arrangement prevailed in this test, and the computer results indicated that under such action, a yet smaller flange width would be effective in resisting loads.

With three acceptable comparisons, it could be said with certainty that for either simple support or cantilever action under symmetric moments, the precast boxes act compositely with the joists, providing an effective flange width of 44 mm, or approximately 25% of the total width of the box, on each side of the joists.

#### 4.4 Parametric Study Using Finite Element Models

Studies of two-way open grid slab systems by Parma (Ref. 4) included a parametric study on the Coefficient of Torsional Efficiency, defined as:

$$t = \frac{M}{\Psi} \frac{x}{EI_b}$$

where  $M$  = sum of a pair of equal applied moments at two corners acting in a vertical plane and parallel to the x-direction (Fig. 42).

$\Psi$  = average rotations at the same two loaded corners.

$x$  = edge to edge span of slab in the x-direction

$E$  = Modulus of Elasticity

$I_b$  = summation of moments of inertia of all sections at mid-span cut by a vertical plane perpendicular to the x-direction.

For a model under pure bending,  $M/EI$  would be equal to  $\Psi/x$  and  $t$  would have a value of 1. On the other hand, a slab under pure torsion would give a zero  $t$ . Any combined action of flexure and torsion would result in a  $t$  value between the two extremes.

Parma studied more than 500 different cases by changing such parameters as the edge conditions; aspect ratio of slab panel  $x/y$ ; number of panels with filler boxes in each direction, and so on. Graphical presentation of each case was provided. Since one particular case of cantilever action with 6 panels in each direction from Parma's study coincided with the slab model studied in this particular work, it was felt that comparisons could be performed for two purposes. With all the flanges eliminated from the beam elements and the torsional stiffness appropriately adjusted, the finite element model should give identical behavior as Parma's open grid model and would serve as a check for the validity of the finite element model. After this was established, the

equivalent flange width of 44 mm was inserted back to the beams, resulting in a model that closely resembled the experimental slab specimen. A parametric study with varying span lengths was then done on this model and a different torsional efficiency coefficient was obtained for each case. All curves obtained from these studies are shown in Fig. 43; they provided some insight into the characteristic of the slab system being studied. From the graph, it may be observed that there was a discrepancy between Parma's model and the open grid finite element model. This could be explained by the fact that Parma's model, similar to the finite element model, was more heavily reinforced at the corners as illustrated diagrammatically in his report. Since Parma did not make an effort to indicate the exact corner reinforcement he assumed for his model, it was unlikely that the corner elements of the slab model under study would contain the same amount of steel. It was this difference in end reinforcements that resulted in diverged end rotations, and thus, the torsional efficiency coefficient between the two models. Nevertheless, the parallel nature of the curves indicated that the two models did have close resemblance and it was obvious that by varying the amount of reinforcement in either model, the two curves could be brought to almost coincide with each other. Judging by the above consideration, it was felt that the finite element model used in this study did properly represent the real structure. A curve for the box panel slab system under study, represented by the described finite element model with 44 mm flange width, was also provided in Fig. 43. It should be pointed out that, as expected, the point on this curve at the  $x/y$

## 5. CONCLUSION AND REMARKS

In summary, all the work carried out in this study is presented as follows: Three basic types of models were tested experimentally. A single reinforced joist without any boxes was subjected to bending test and was loaded to failure. Two strip models, each with different reinforcements, were then tested. A strip model included two parallel reinforced joists binding a row of six hollow boxes between them. All filler boxes were precast in halves using plexiglass molds. A square slab model, six boxes on each side, was then tested in two phases. First, end moments simulating the effect of sidesway within elastic range were applied to the specimen. Four sets of such tests were performed, each with a different combination of loading mode and support condition. The second phase was an ultimate test during which the simple supported slab was subjected to vertical design service load as well as equal increasing end moments at all corners. The test was ended when two corners broke off completely.

From the test results of the joist and strip tests, theoretical I-beams, in which the webs were equal to the sum of the solid stems and box walls of the strip models, was so constructed that their bending stiffnesses were equal to the experimental specimens'. The average flange width of these I-beams gave the approximate effective width of the box sections. Using finite element analysis, a theoretical model of the slab specimen was obtained. The finite element model was simplified to a two-way open grid system and through a trial and error

ratio of 1 coincided with the actual test result of the slab model. The fact that such slab systems had smaller coefficients than it's open grid counterpart by no means implied that the former structure was weaker. On the contrary, the box panel system did provide smaller deflections. A smaller torsional efficiency coefficient simply indicated that a higher fraction of recorded rotations was caused by torsional effect. Thus, an extremely high torsional stiffness would minimize torsional rotations and provide a coefficient close to 1, whereas a model with relatively low torsional stiffness would give a higher proportion of end rotation due to torsional effect and result in a smaller coefficient. It was felt that the true physical meaning of the torsional efficiency coefficient was not significant in this study. So long as the curve was established correctly and could truly represent the panel box slab system, one would be able to use it as a design chart for such structures.

A final finite element study was conducted in order to determine an equivalent solid slab that had the same stiffness as the slab model under study. SAP IV computer result showed that a solid slab with a thickness of 44.7 mm would show similar characteristics as the experimental model which had a total thickness of 72 mm.

process, the equivalent flange width to the effective box section in the slab model was determined. With such section established, a design curve for the 6 x 6 slab model was determined using Parma's study on coefficient of torsional efficiency.

Combining the result of all the analyses, it could be concluded that for symmetric loading, the described slab system could be treated as a two-way joist open grid structure. The effective sections of the joist should be that of an I-beam with the web section identical to that of corresponding interconnecting joist with the box wall and the flange width on each side equal to 25% of the box panel width.

Further work could be continued for this study. The ultimate load for the slab model had not been determined due to a premature failure at the loading corners. Since the slab model was still intact, these corners could simply be repaired and the ultimate load test then be completed. From the described experience, it is advised that test models built for any future work shall have the protruding corners at least as heavily reinforced as the solid corner panels, thus avoiding similar undesirable breakage.

The design curve the the slab model in Fig. 38 was based on the assumption total a 0.044 m flange width was applicable for a slab of any aspect ratio. Since this assumption had not been verified by any actual test, future study could be started off by performing experimental load tests on slab models of different dimensions in order to check the validity of the curve established in this study. On an even wider basis, a numerous number of slab specimens should be experimentally



tested so that a series of curves, each one depicting a group of slabs with the same arrangement and equal number of box panels but with different aspect ratios. Through the use of an appropriate curve, deflections of slabs of known dimension could be determined by reading off at the known moment level. It was hoped that with the availability of these design curves, a new dimension of design would be open in this field.



6. TABLES

	Amount by Weight (N)	Percentage by Weight
Sand	144	63.0
Cement	53	23.1
Water	32	13.9

TABLE 1: Mix of filler boxes for 1 m<sup>3</sup> of concrete

Sieve Size	Percent Passing -
30	100
50	41.2
100	9.0

TABLE 2: Gradation of sand for filler box mix

	Amount by Weight (N)	Percentage by Weight
Sand	144	65.2
Cement	48	21.7
Water	29	13.1

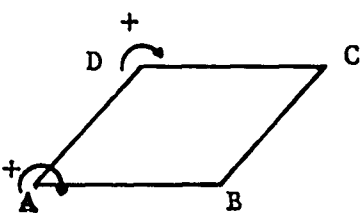
TABLE 3: Mix of joists and slab for 1 m<sup>3</sup> of concrete

Sieve Size	Percent Passing
8	100.0
16	84.5
30	65.8
50	28.5
100	4.6

TABLE 4: Gradation of sand for the slab specimen

Diameter (mm)	Area (mm <sup>2</sup> )	Yield Strength (MPa)
3.4	9.08	293
2.75	5.94	293
2.0	3.14	293
1.27	1.27	293
0.74	0.43	516

TABLE 5: Properties of steel reinforcements



Test	Support Condition	Applied Load
1	B, C fixed A, D free	Equal positive moment at A and D and D
2	B, C fixed A, D free	Equal positive moment at A and D Equal upward force of 177.8 N at A and D
3	B, C, D fixed A free	Positive moment at A
4	All corners simple supported	Equal positive moments at A and D

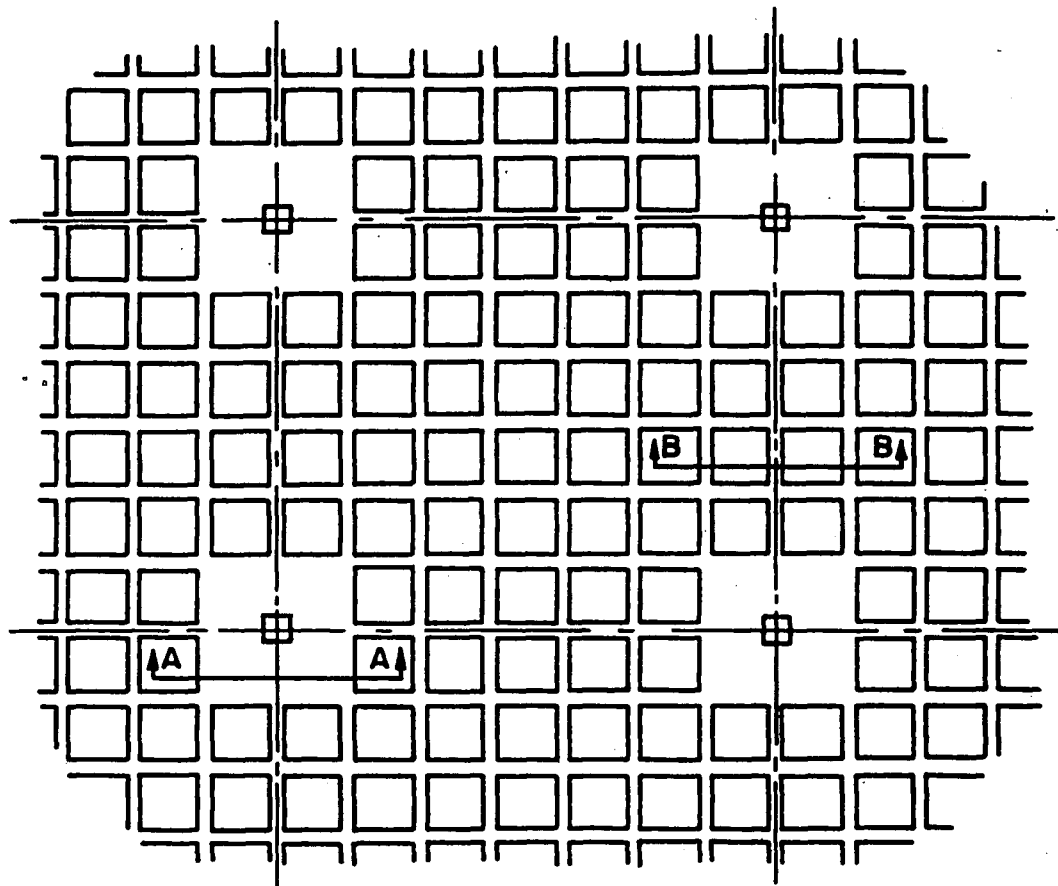
All tests were repeated with all moments, but not concentrated loads, reversed.

TABLE 6: Elastic load tests performed on slab specimen

Test	Rotational Stiffness (N-m)	Carry Over Factor
1	98800	-1
2	136700	Undetermined
3	113900	Undetermined
4	211600	0.63

TABLE 7: Stiffness characteristics of slab specimen determined from elastic tests

7. FIGURES



Plan View

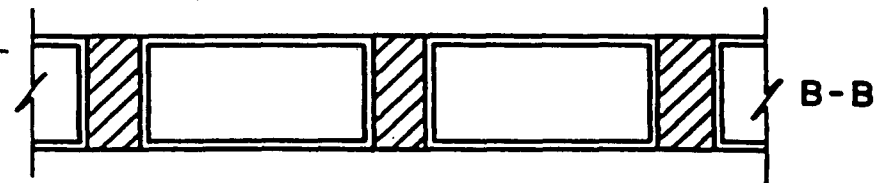
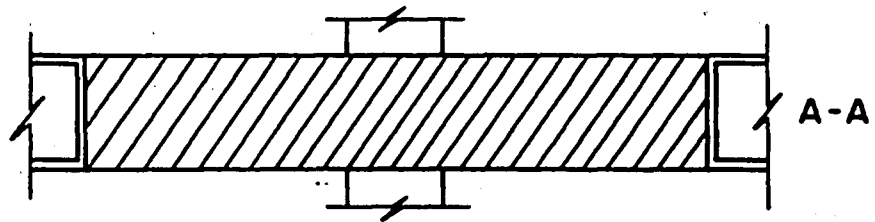


FIG. 1 - Typical Example of a Column Grid System

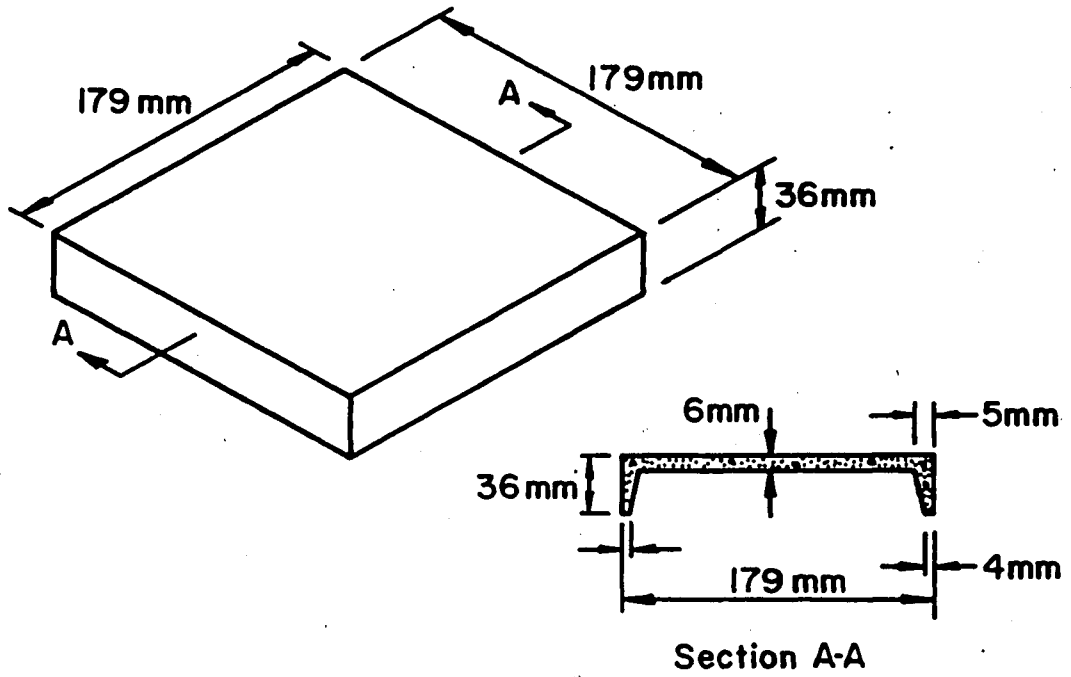


FIG. 2 - Isometric View And Dimensions Of A Fill Box

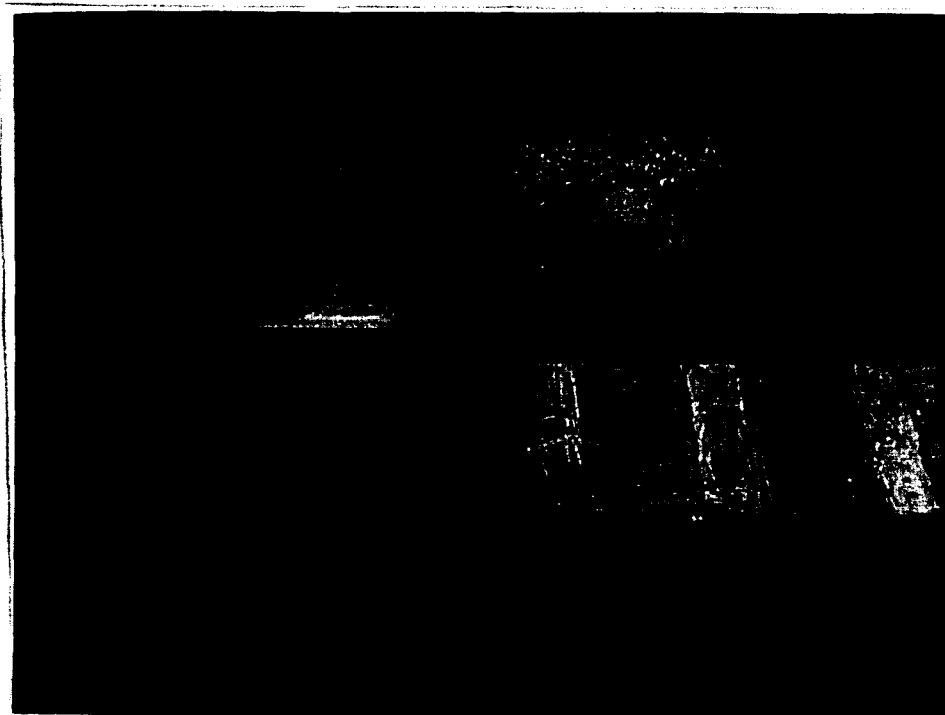


FIG. 3 - Plexiglass Mold For Filler Boxes

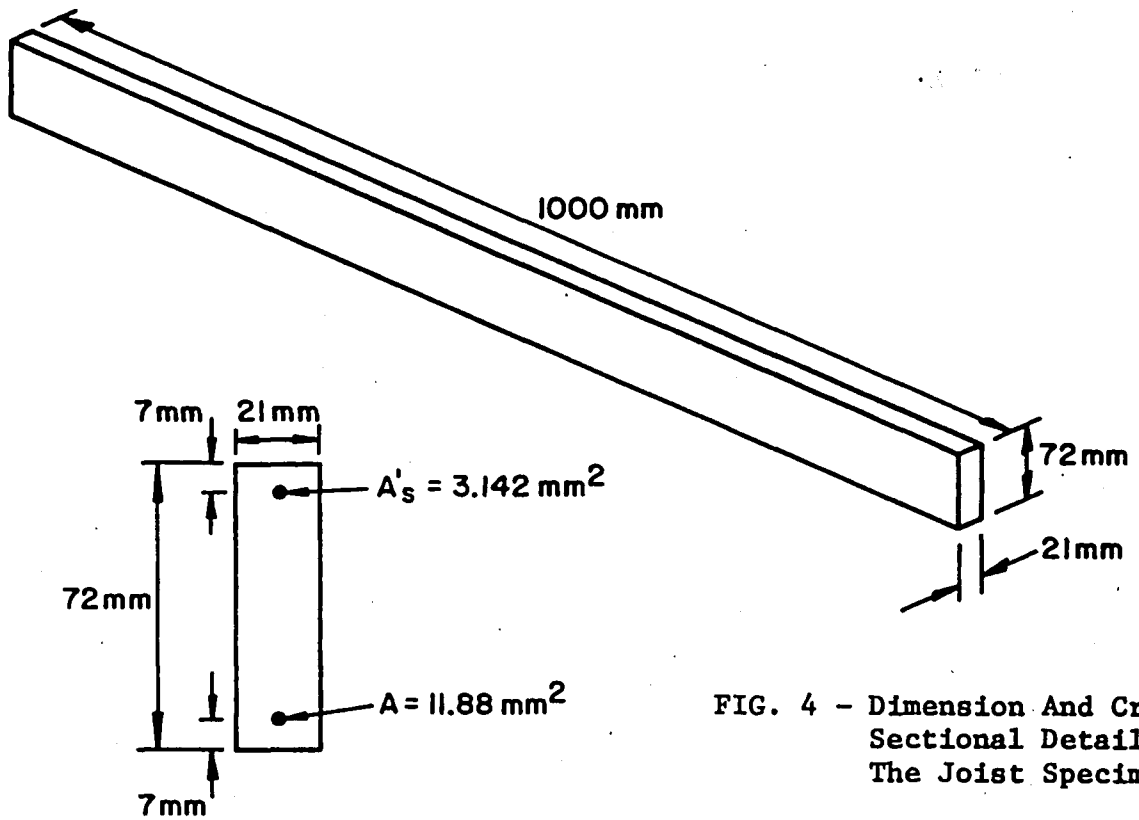


FIG. 4 - Dimension And Cross-Sectional Detail Of The Joist Specimen

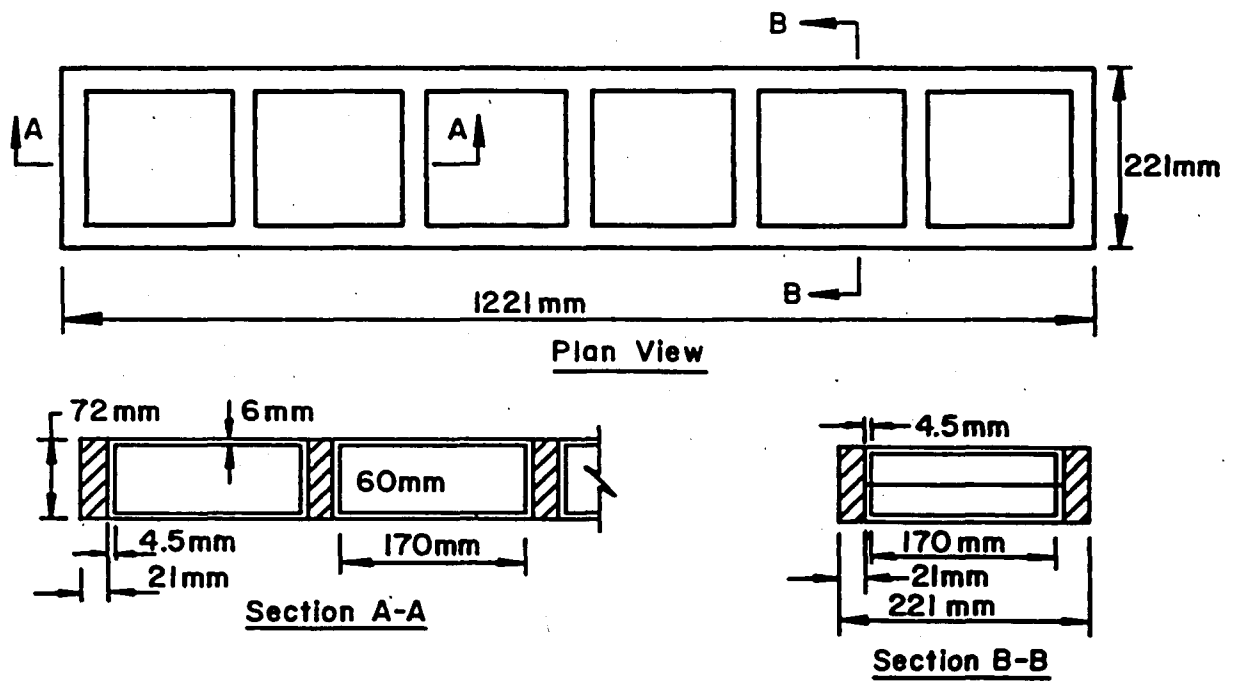


FIG. 5 - Dimension And Cross-Sectional Detail Of The Strip Specimen



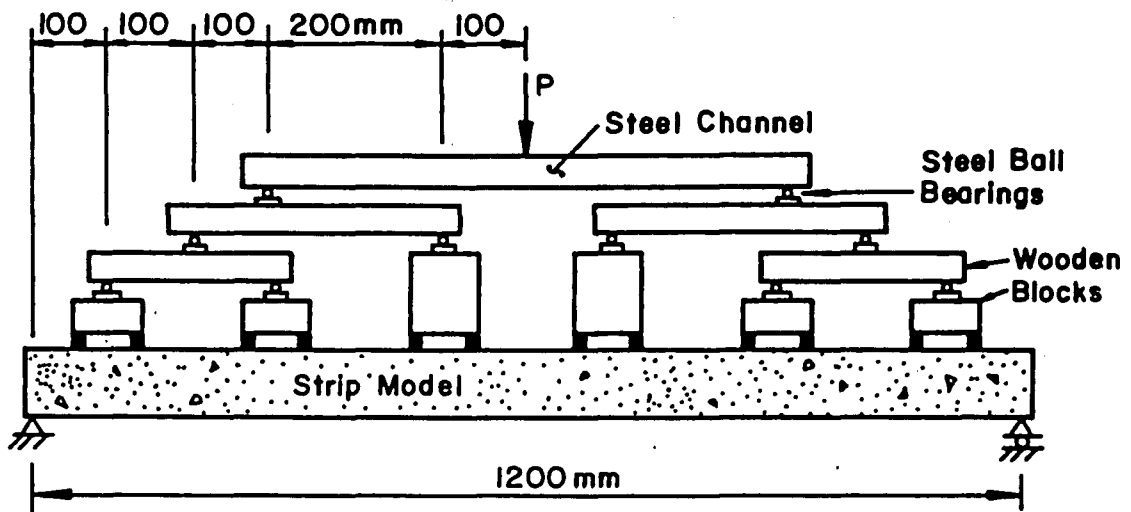


FIG. 6 - Schematic Setup For The Strip Specimen

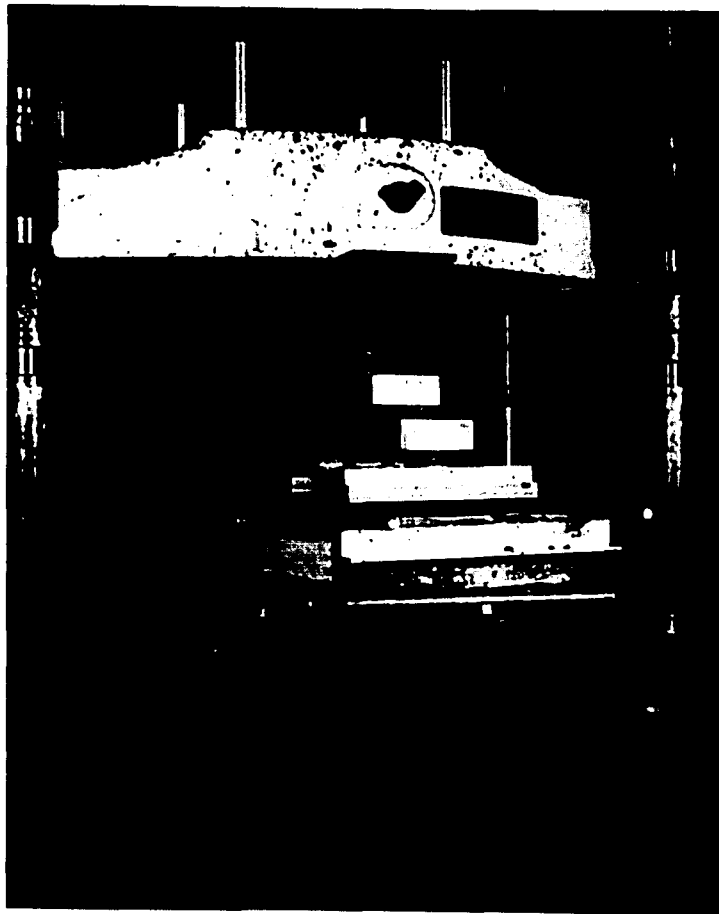


FIG. 7 - Test Setup For Strip Specimen

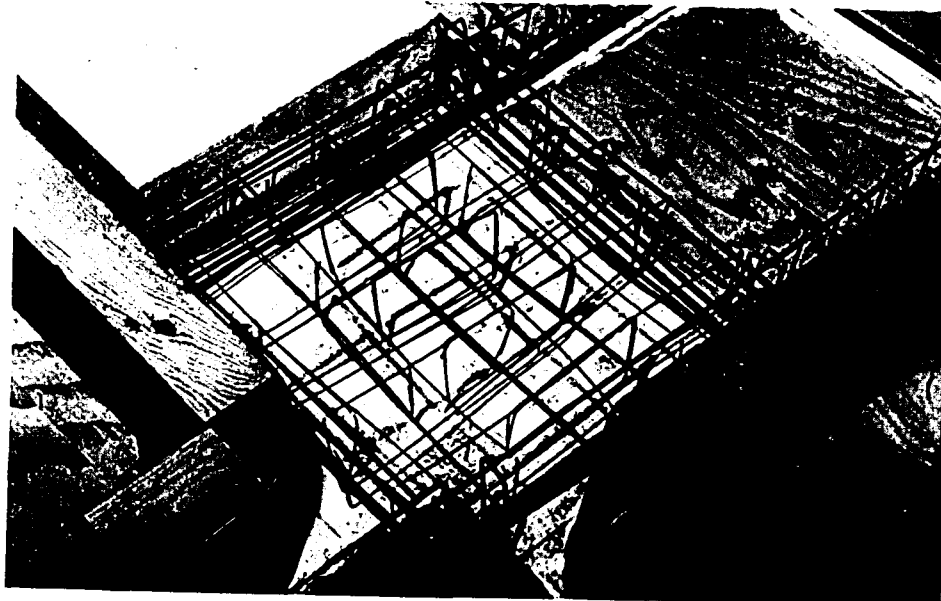


FIG. 8 - Additional Reinforcement In Solid Corner Panel

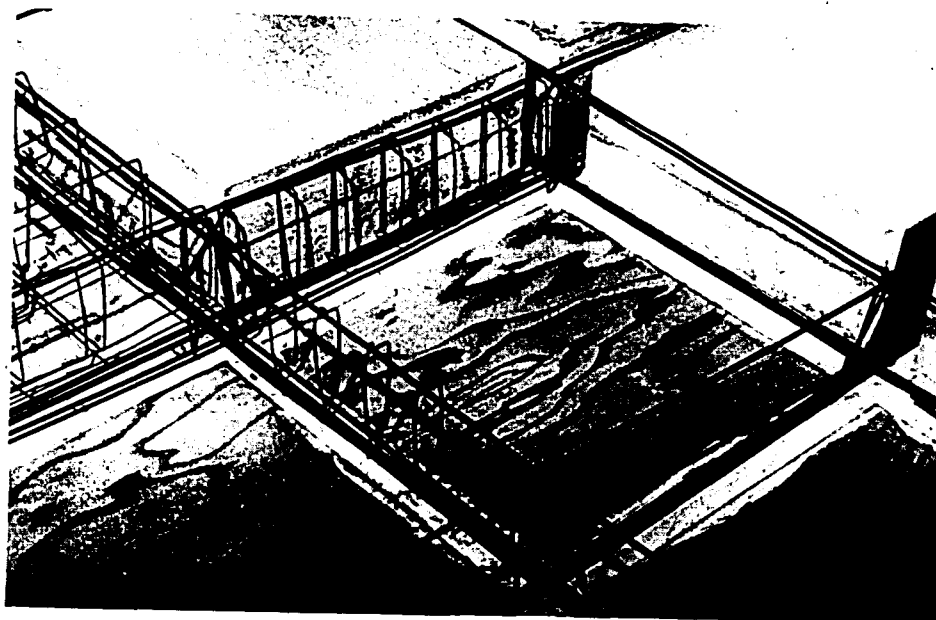


FIG. 9 - Vertical Stirrups For The Outer Joists

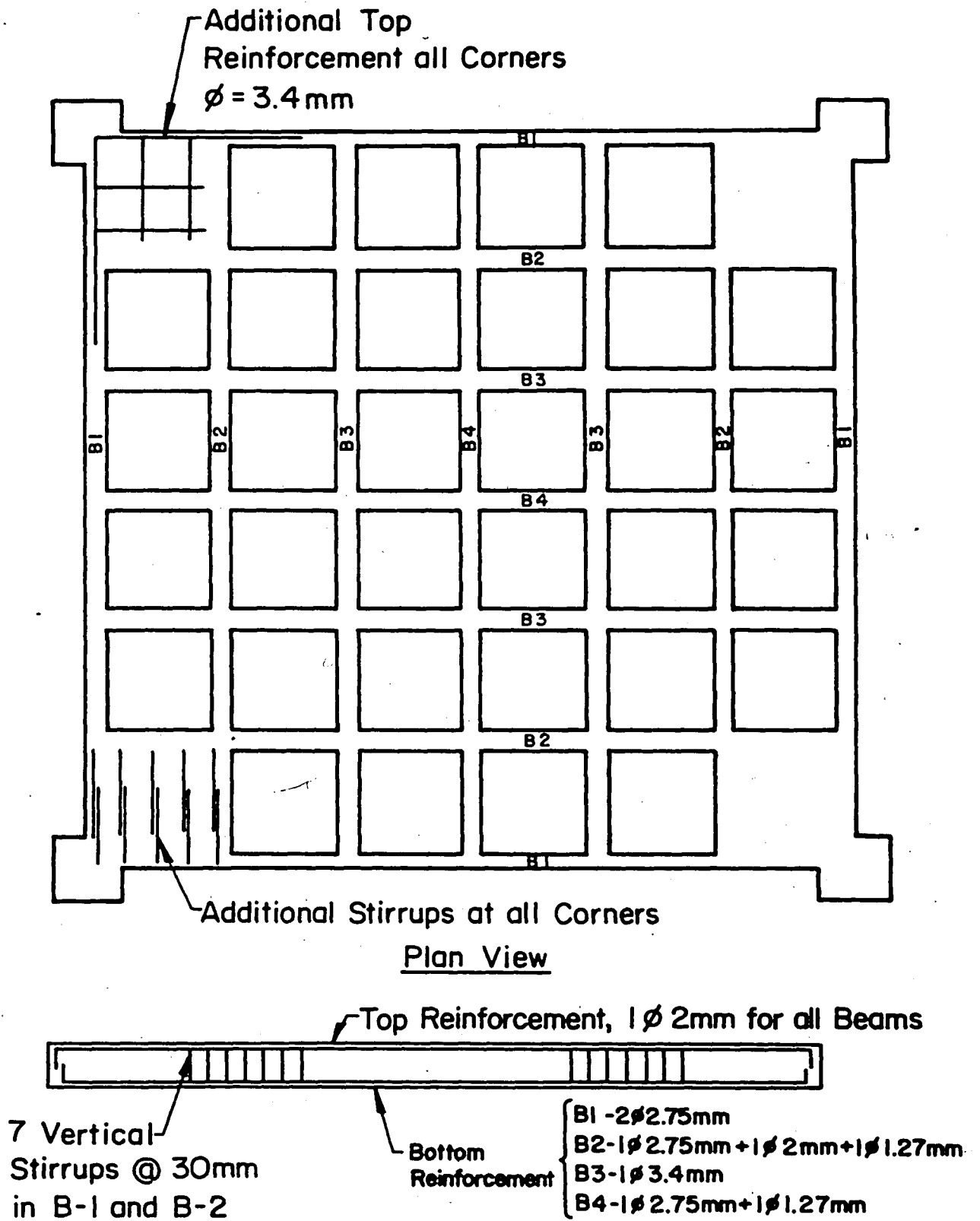


FIG. 10 - Design Detail Of The Slab Specimen

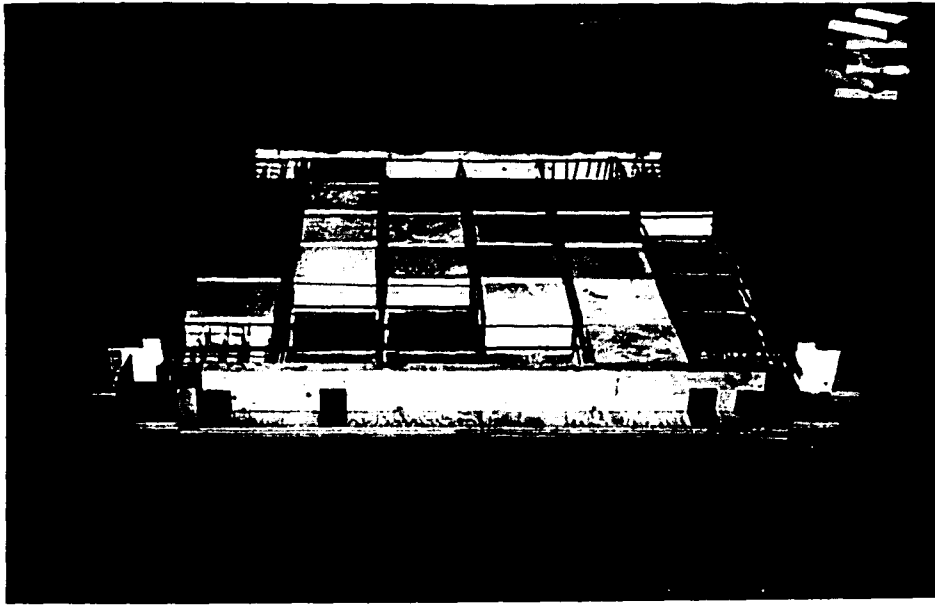


FIG. 11 - Formwork For Slab Specimen Before Casting

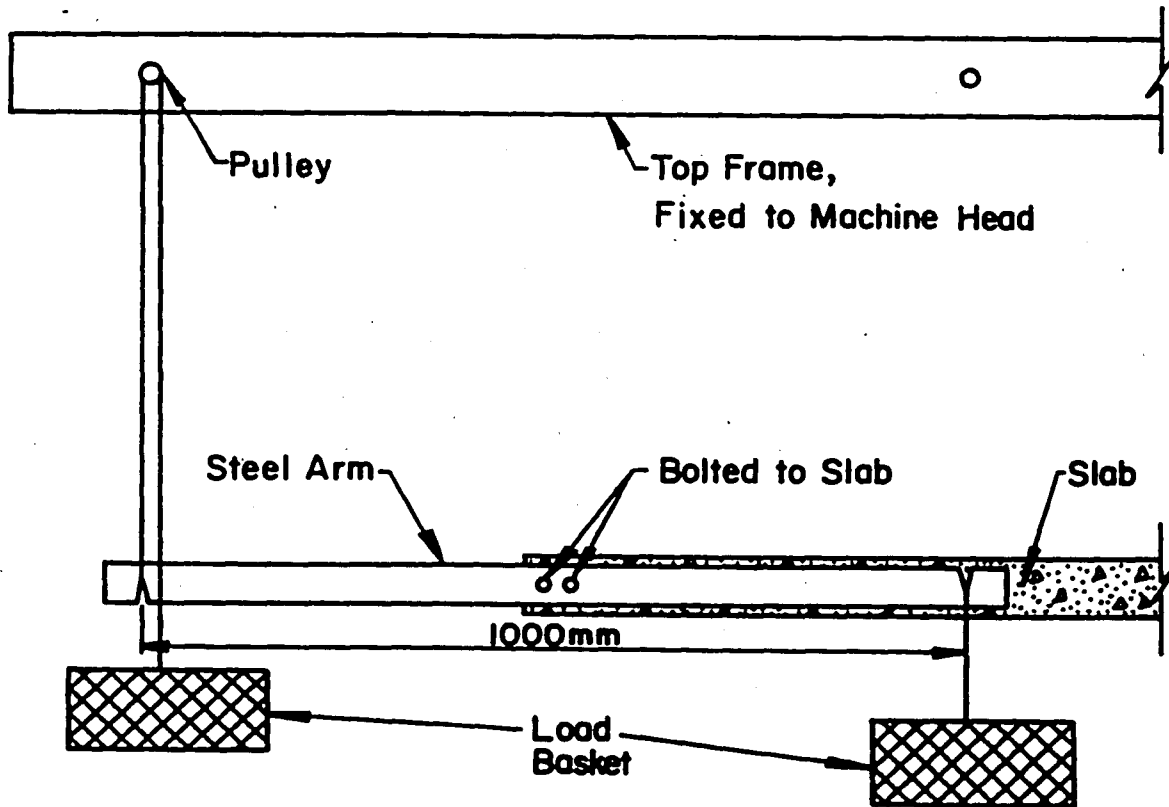


FIG. 12 - Schematic Setup For Moment Application

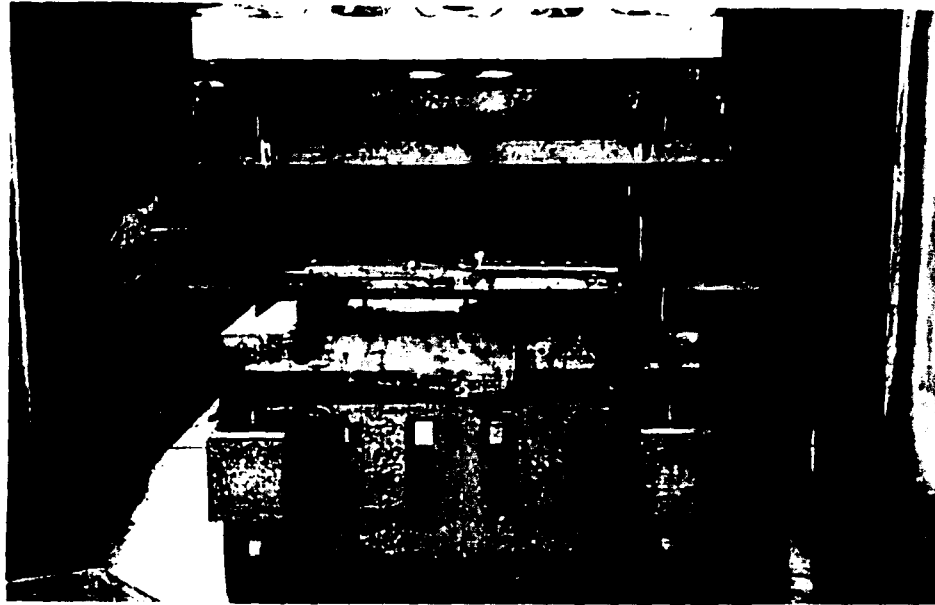


FIG. 13 - Elastic Test Setup For Slab Model

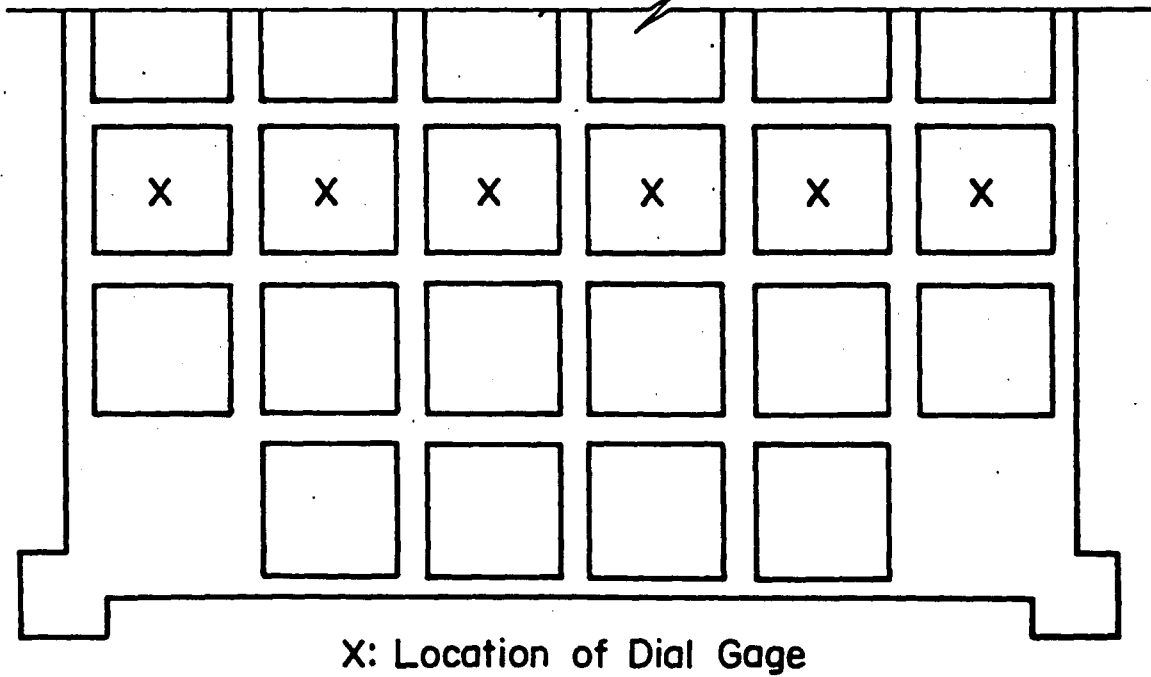


FIG. 14 - Location Of Dial Gages For Elastic Tests

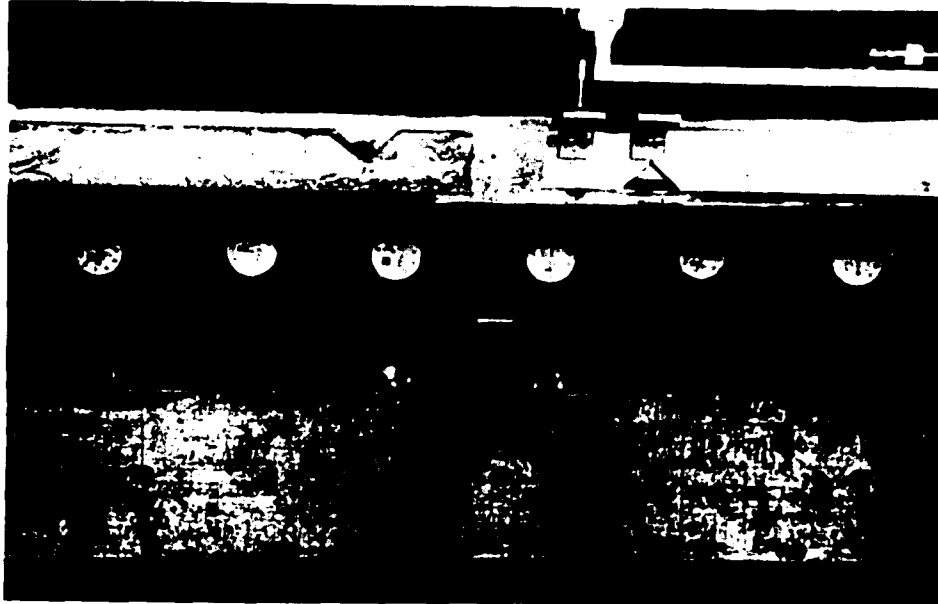
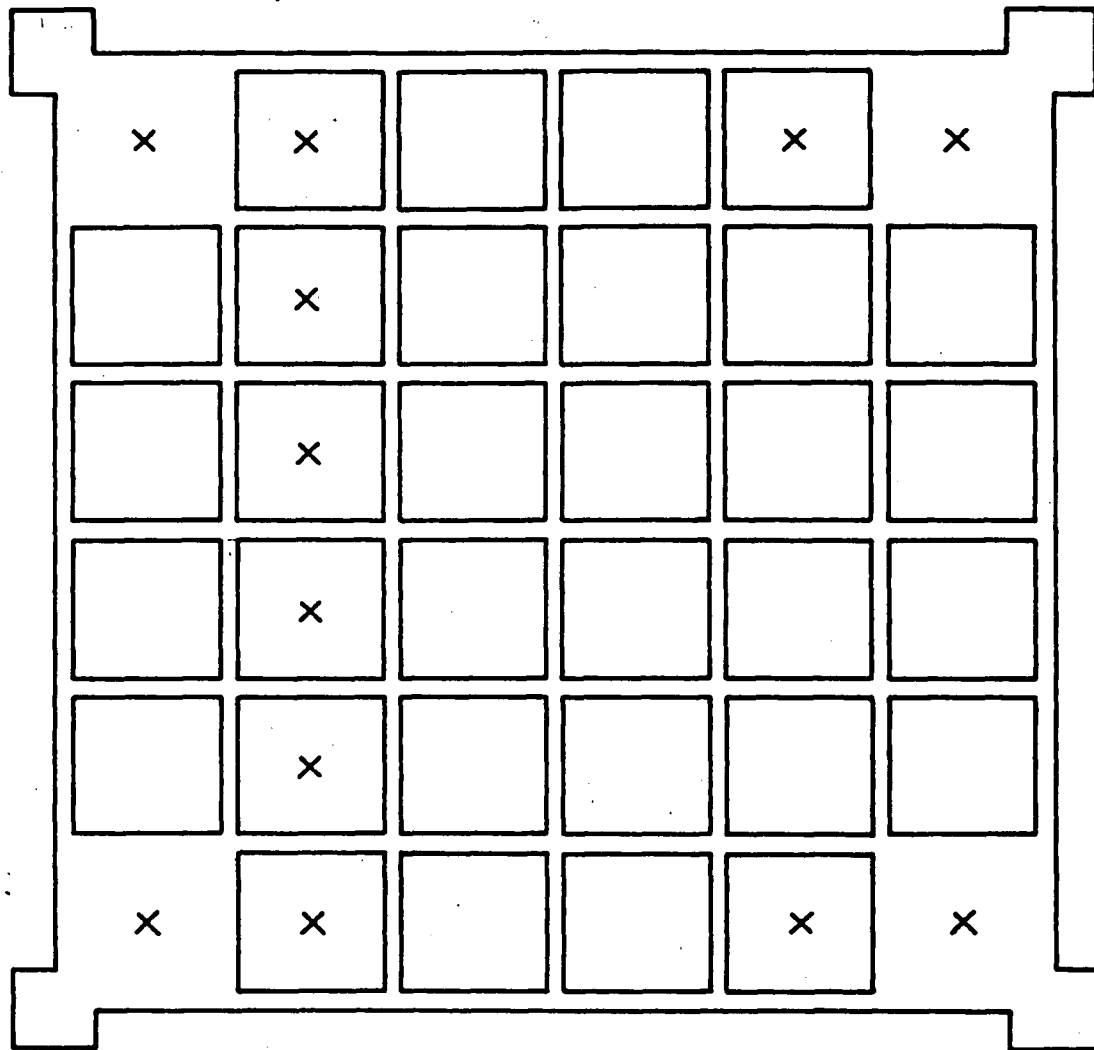


FIG. 15 - Dial Gages Setup For Elastic Tests



FIG. 16 - Rotation Gages Used For Slab Test



X Dial Gage Location

FIG. 17 - Location Of Dial Gages For The Ultimate Load Test

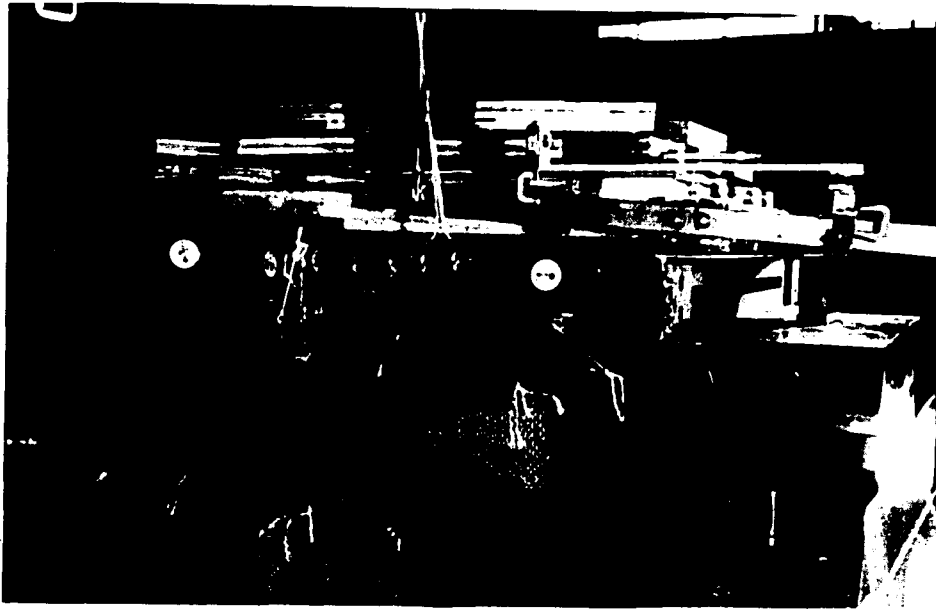


FIG. 18 - Instrument Setup In The Ultimate Load Test



FIG. 19 - First Layer Of Loading Device On The Slab Model



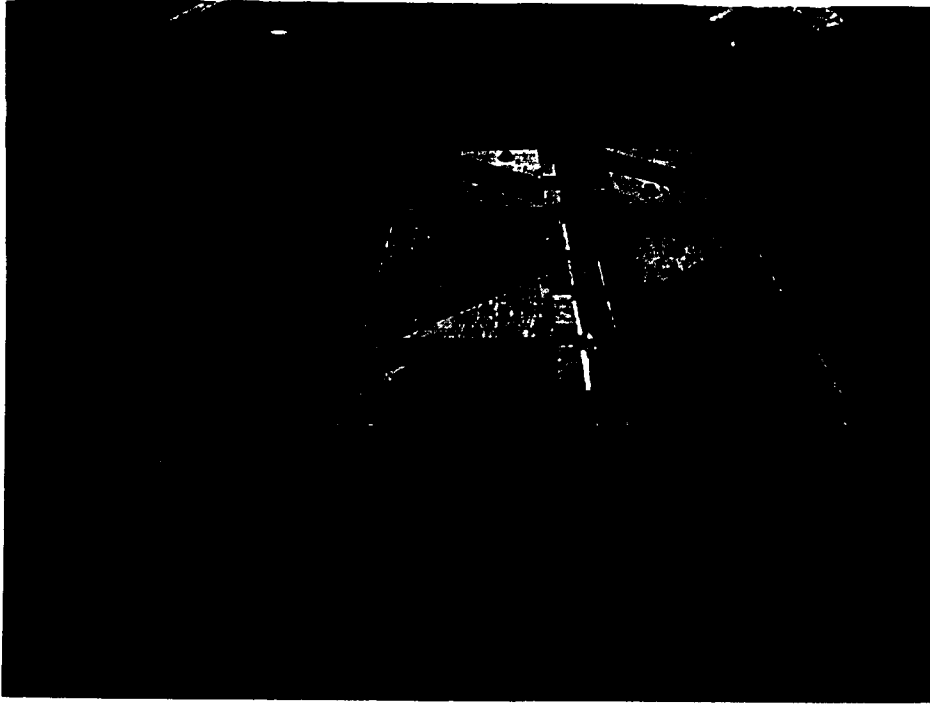


FIG. 20 - Second Layer Of Loading Device

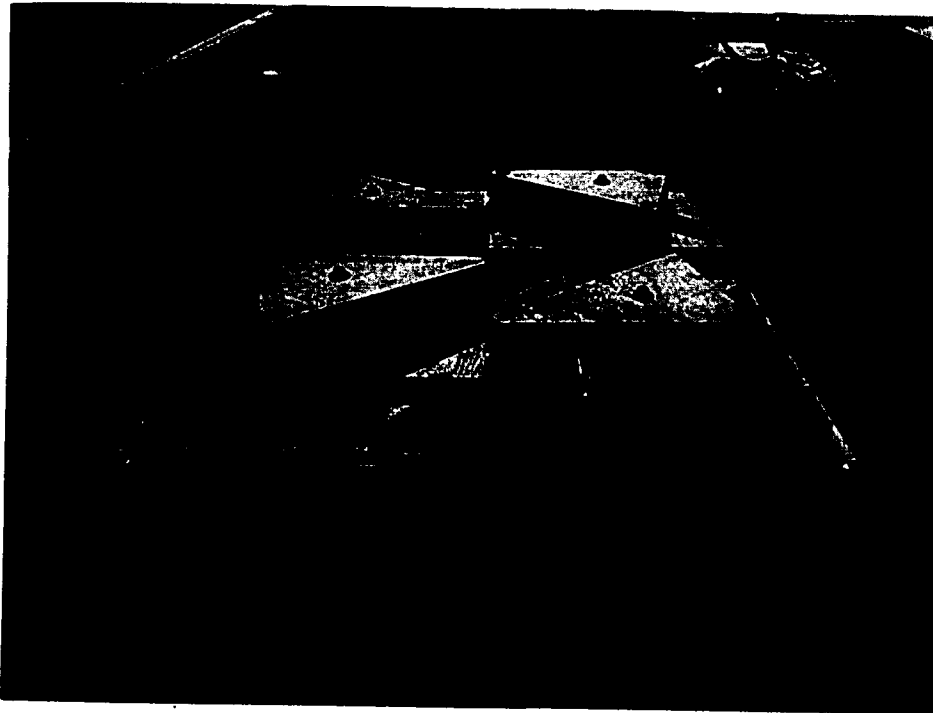


FIG. 21 - Final Layer Of Loading Device

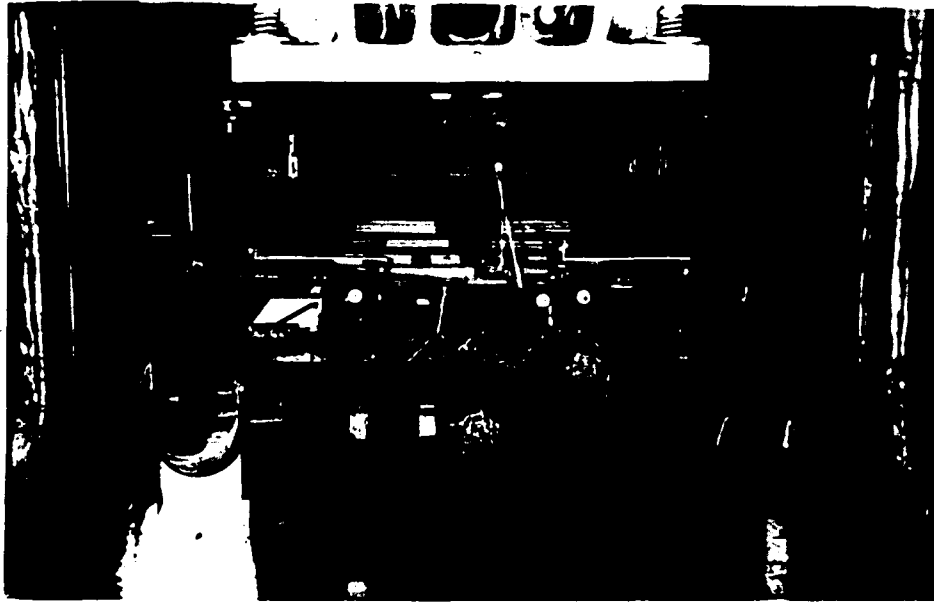


FIG. 22 - Complete Loading Setup For The Ultimate Test Of The Slab Specimen

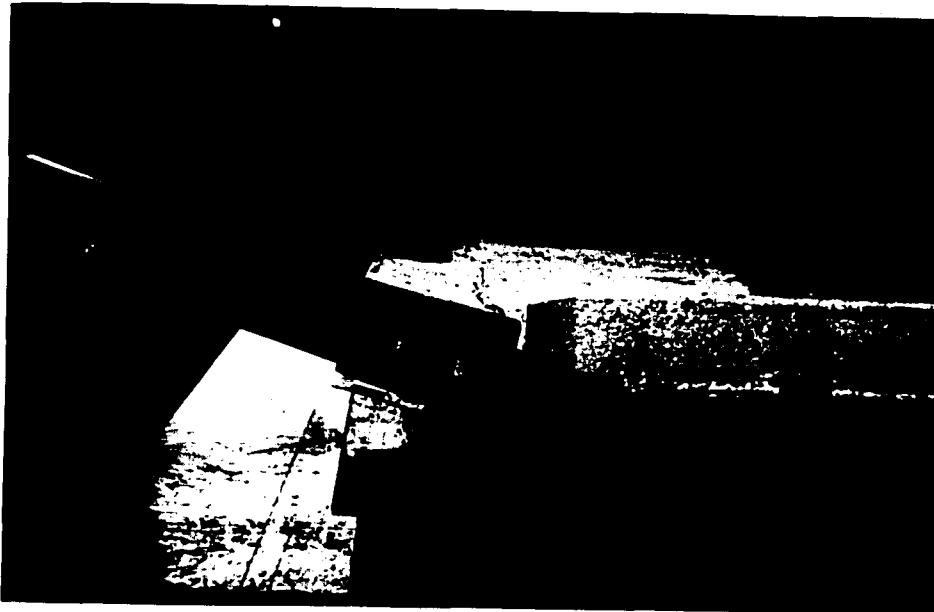


FIG. 23 - One Loading Corner Broke Off From The Slab Model At An Applied Moment Of 444.4 N-M

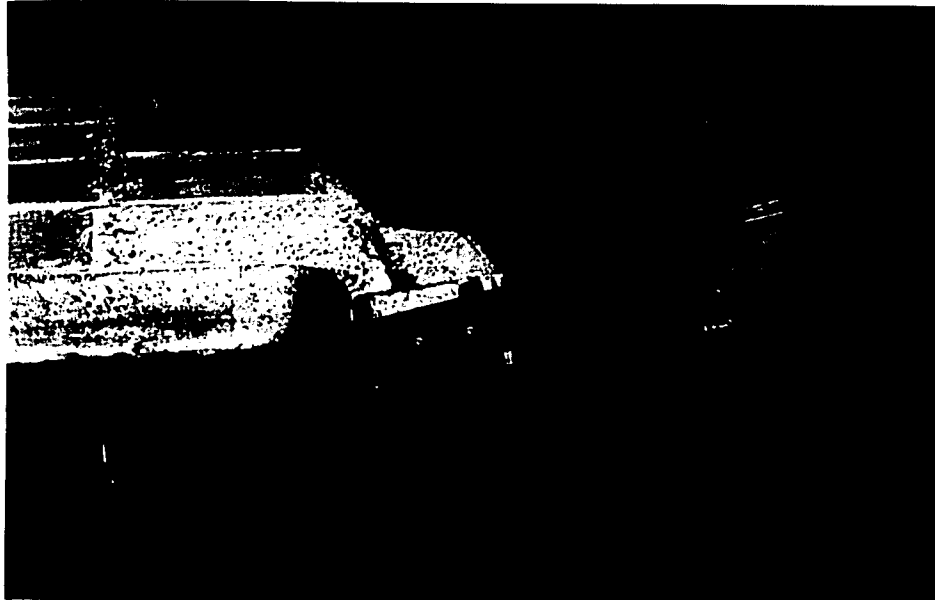


FIG. 24 - Similar Failure Occurred At The Other Corner At 533.3 N-M

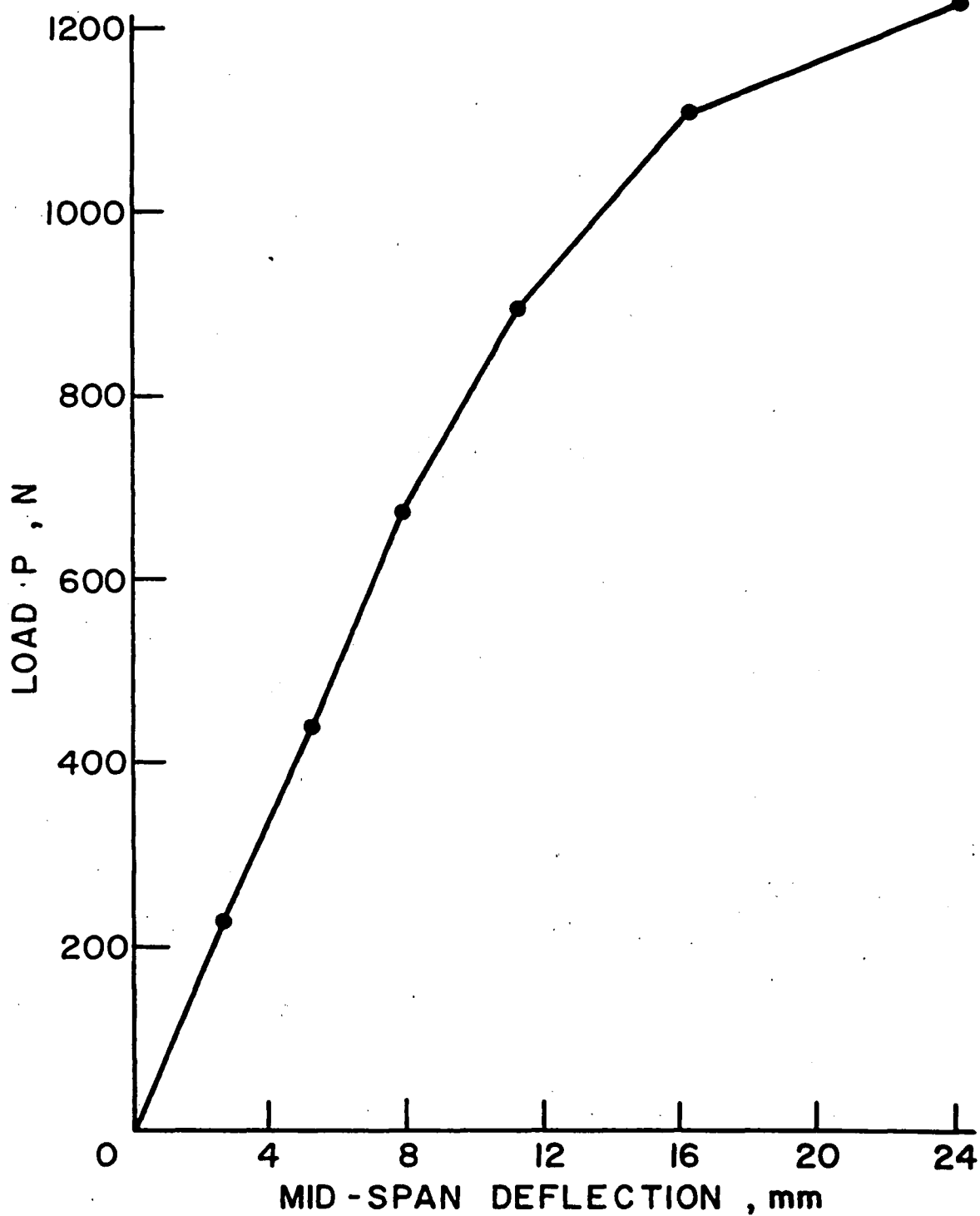


FIG. 25 - Load-Deflection Curve For Mid-Span Of Joist Specimen

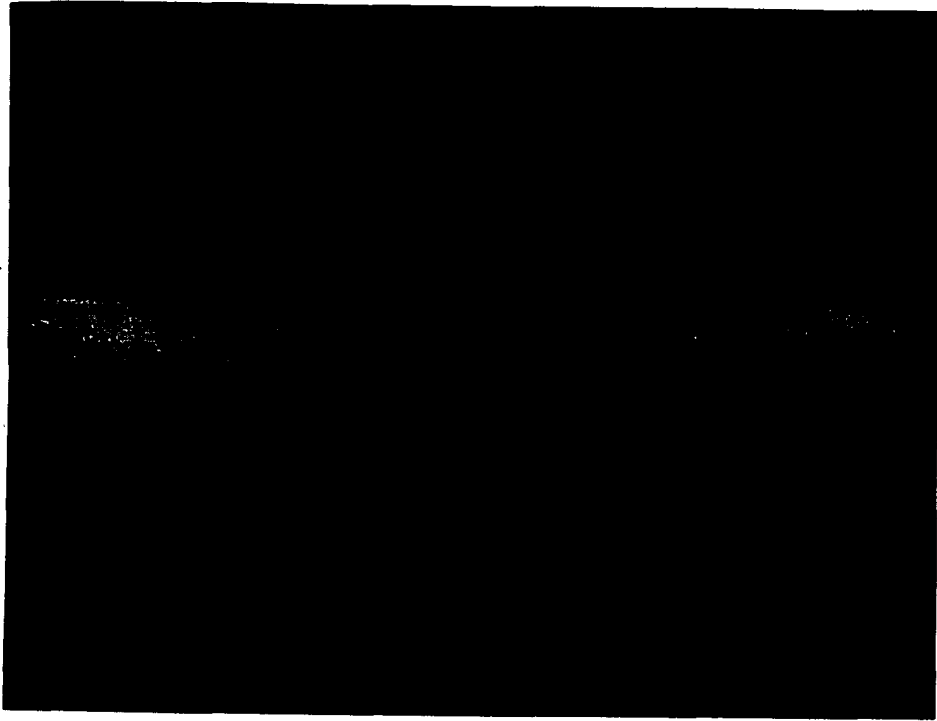


FIG. 26 - Joist Specimen After Ultimate Failure

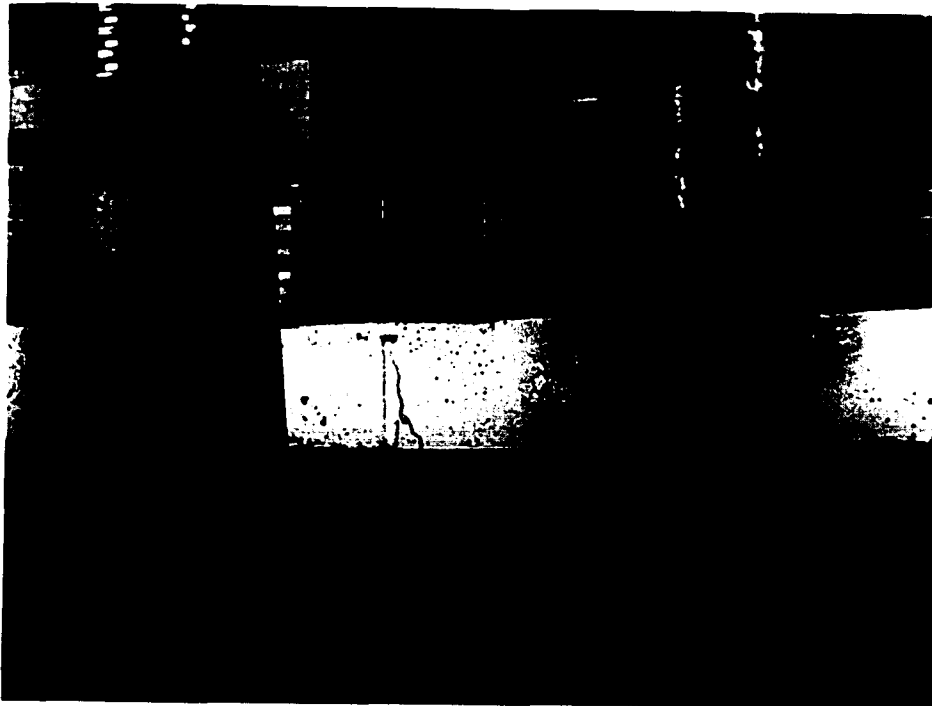


FIG. 27 - Mid-Span Crack Of Strip Specimen Before Ultimate Failure

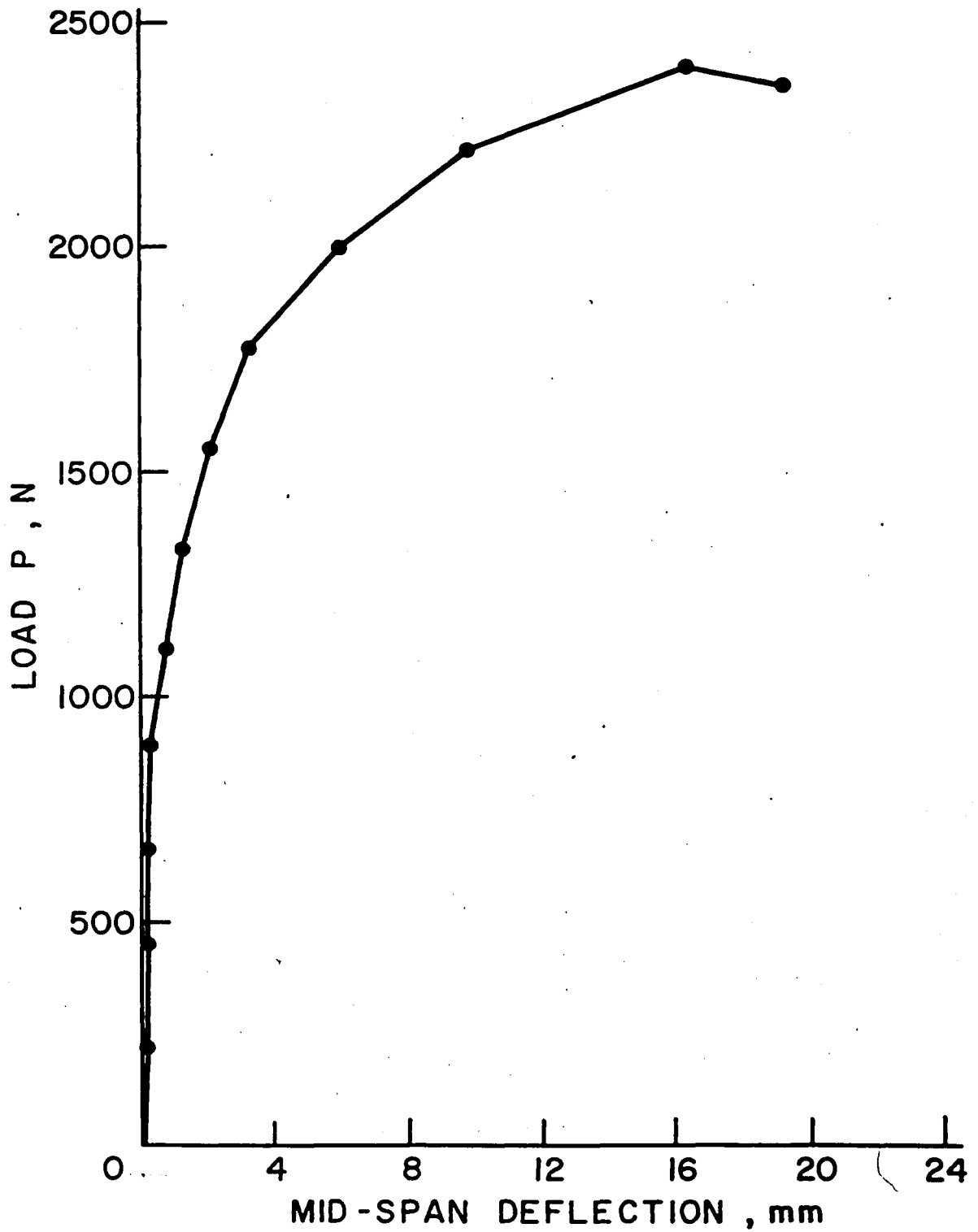


FIG. 28 - Load-Deflection Curve For Mid-Span Of The First Strip Specimen

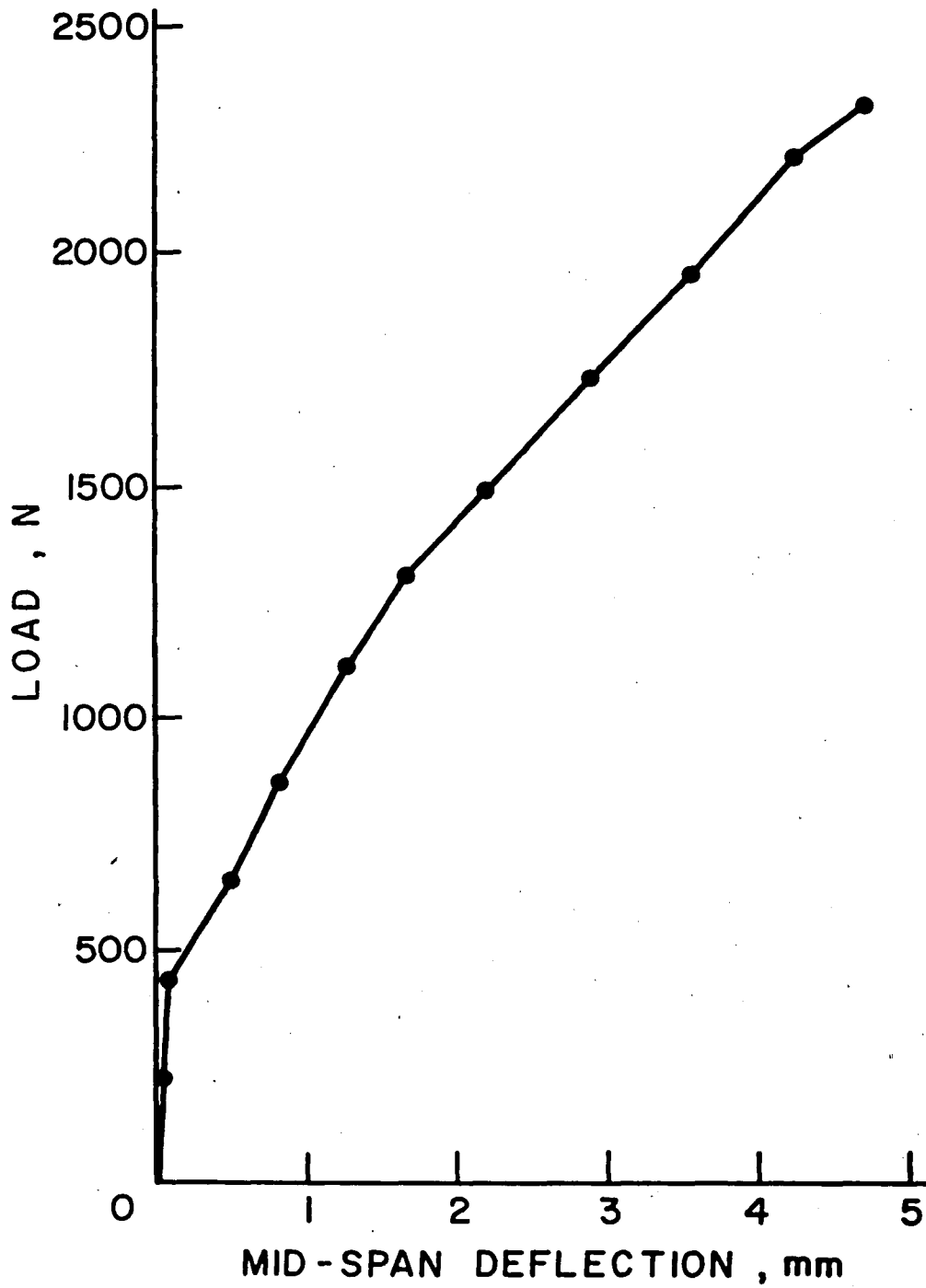


FIG. 29 - Load-Deflection Curve For Mid-Span Of The Second Strip Specimen

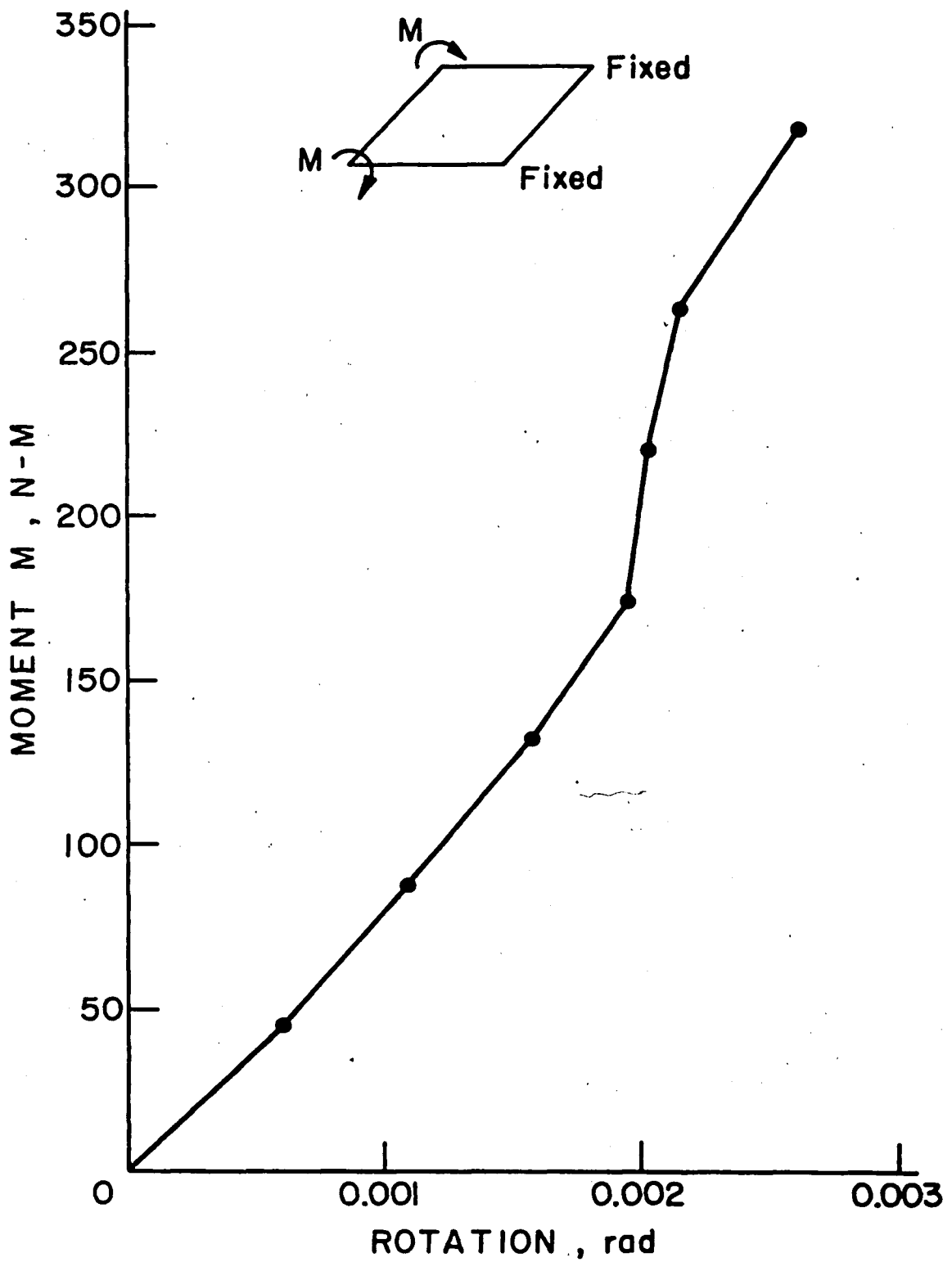


FIG. 30 - Average Rotation At Loaded Corners For Test 1



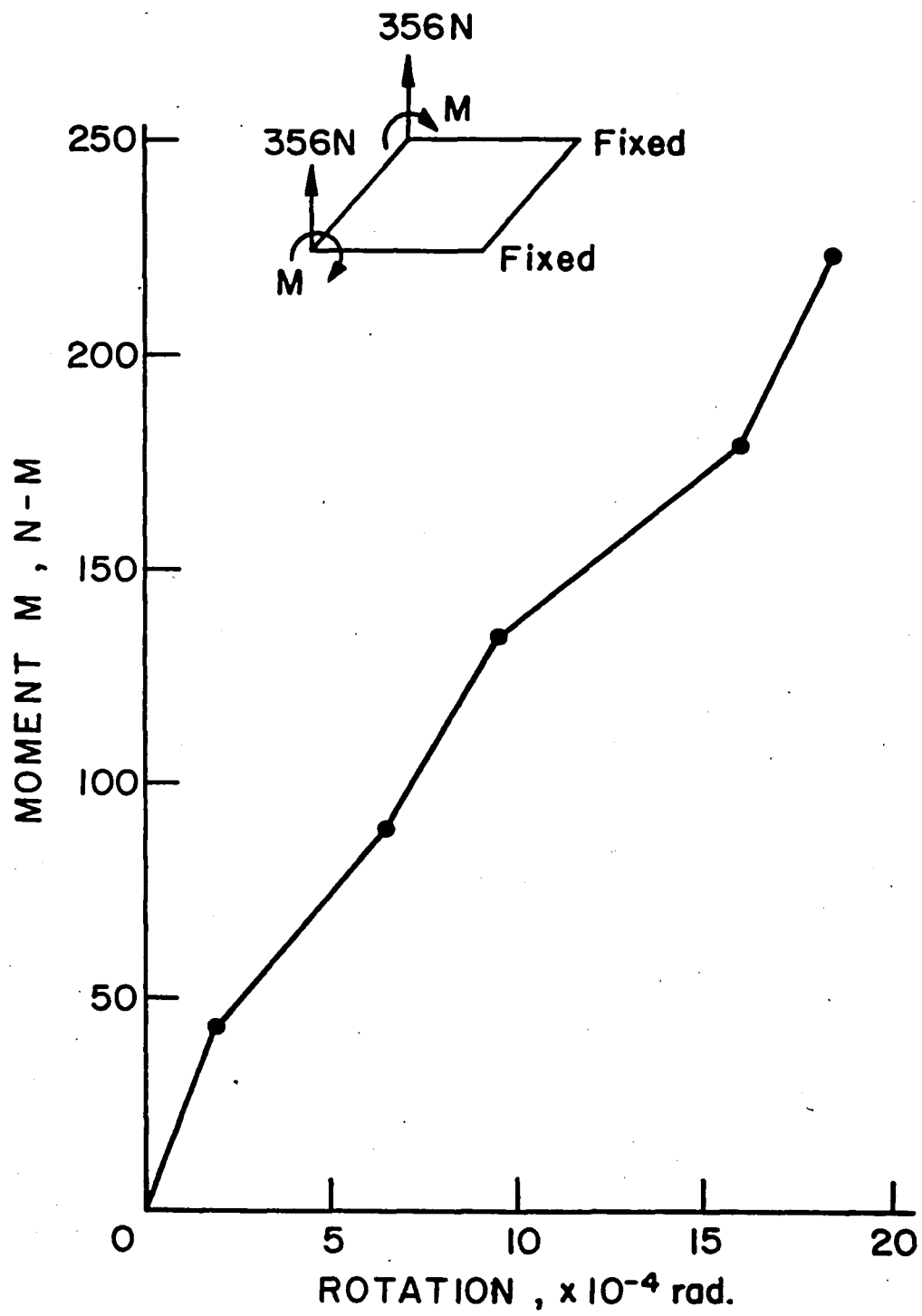


FIG. 31 - Average Rotation At Loaded Corners For Test 2

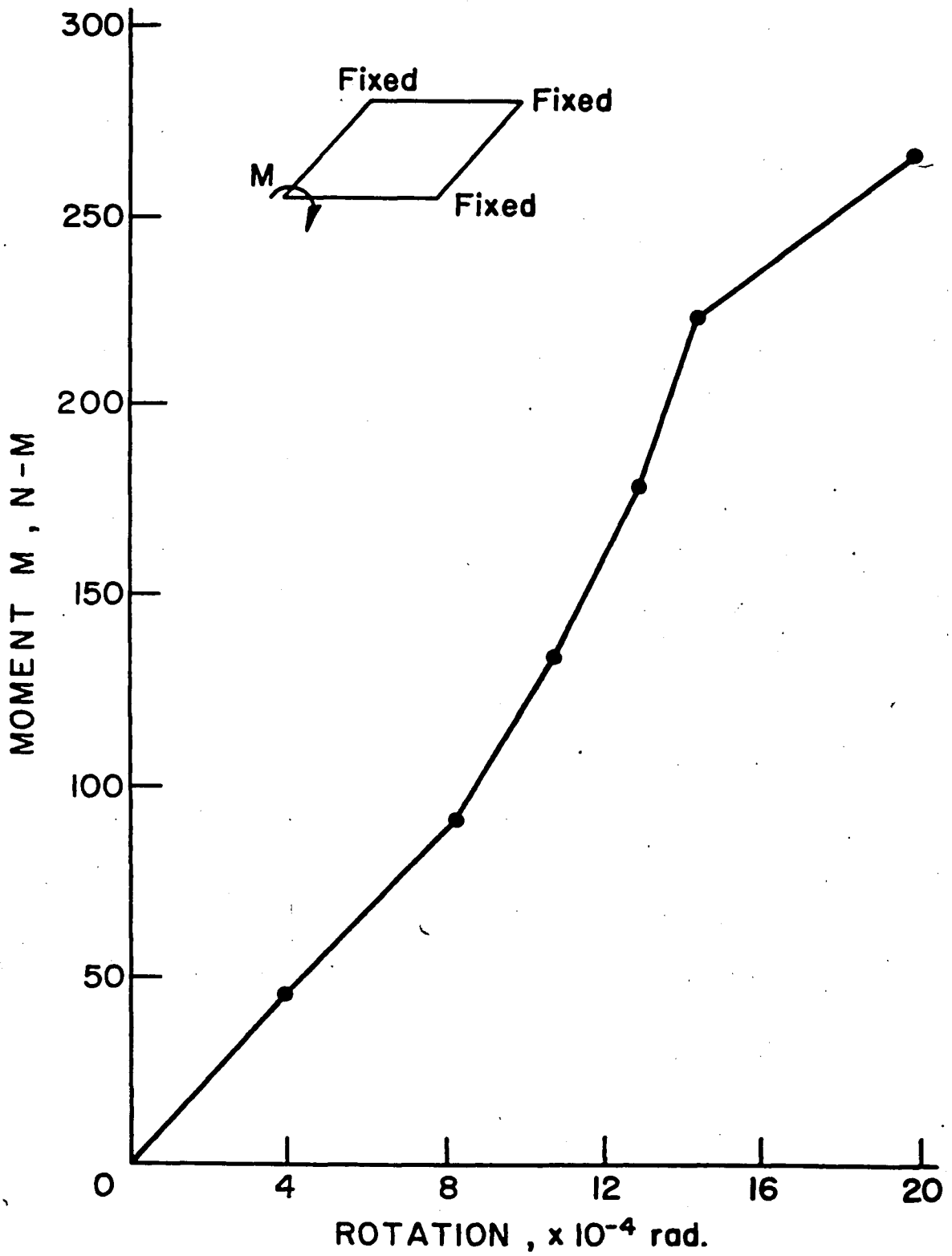


FIG. 32 - Rotation At Loaded Corner For Test 3

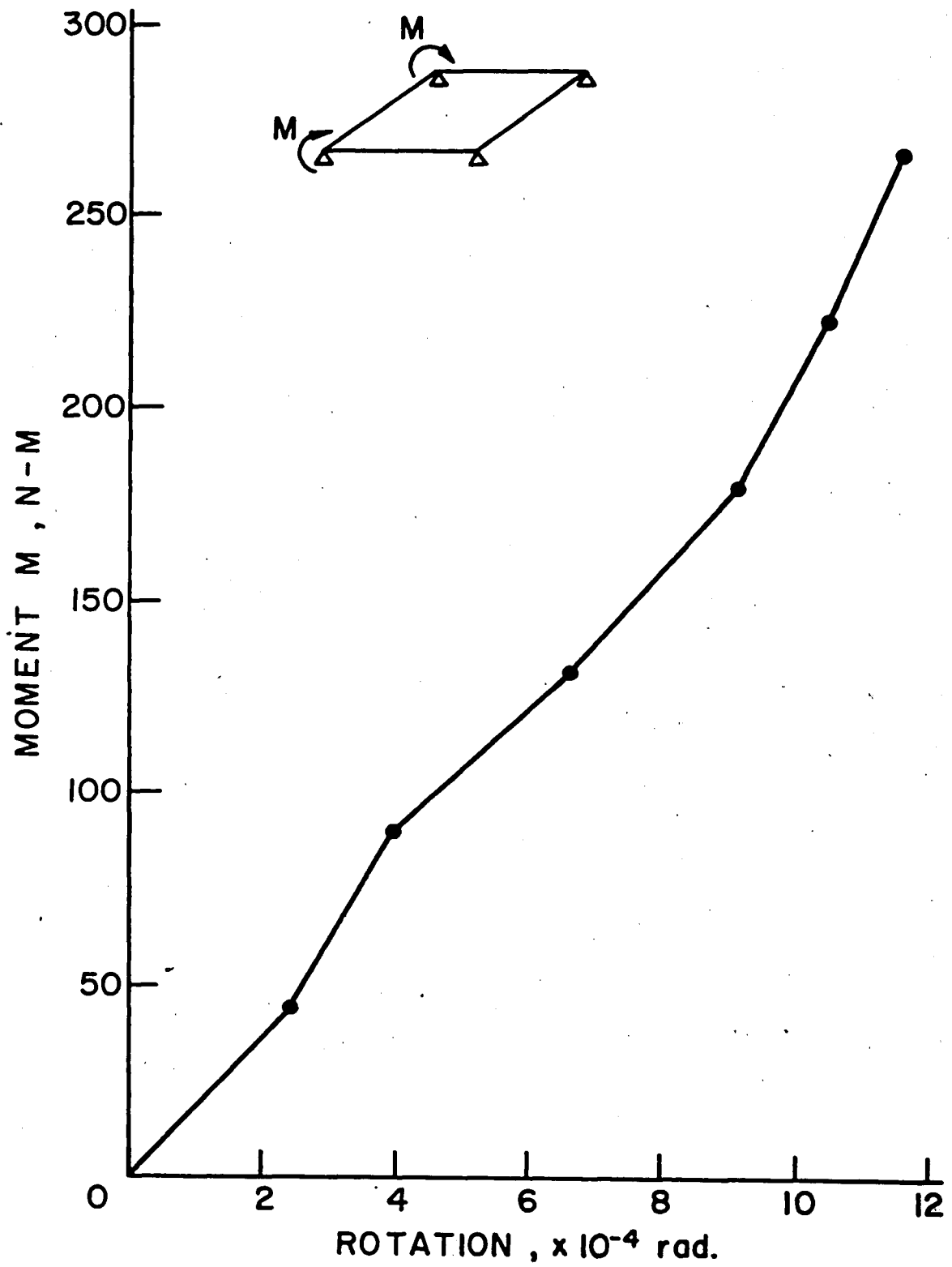


FIG. 33 - Average Rotation At The Loaded Corners For Test 4

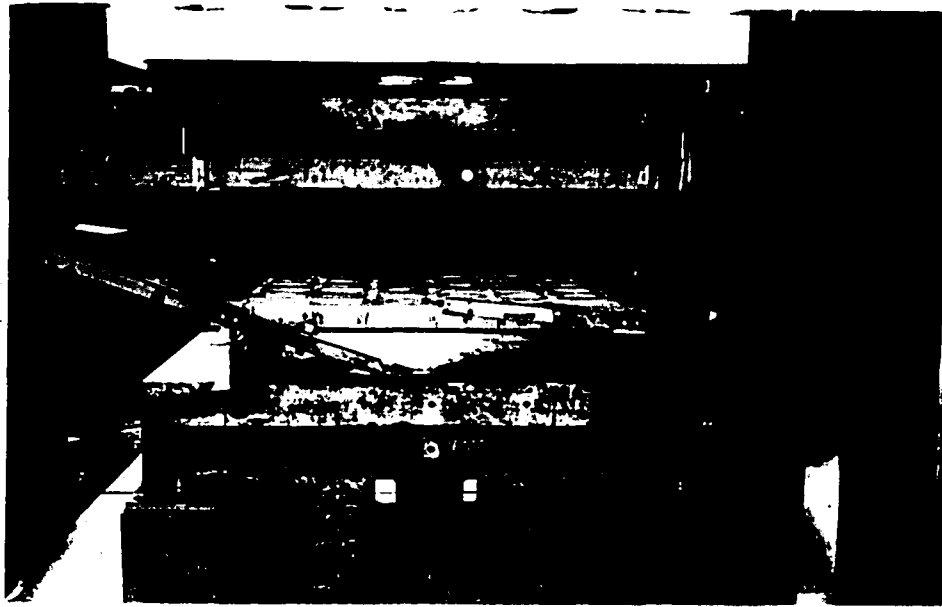


FIG. 34 - Slab Specimen At Completion Of All Load Tests

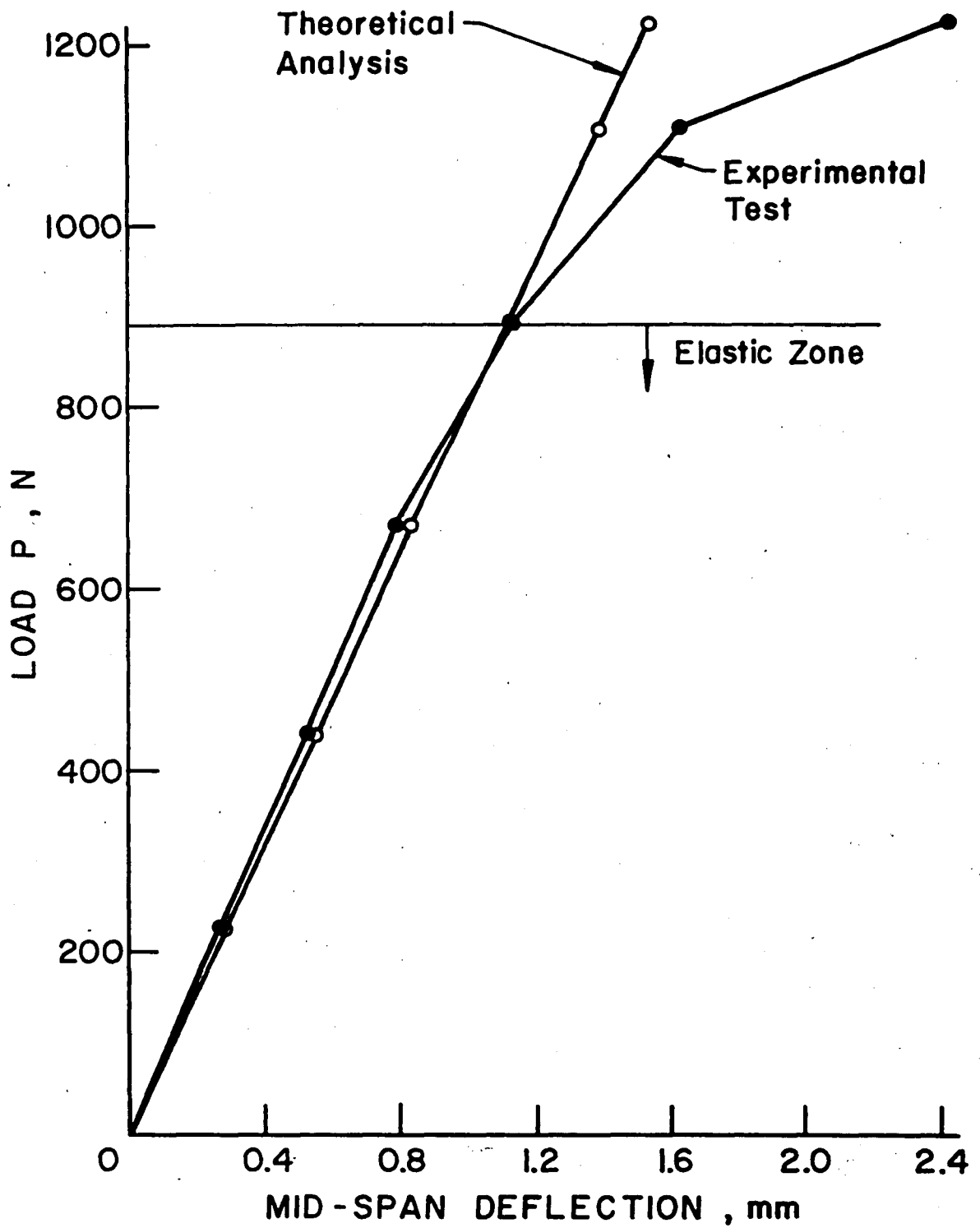


FIG. 35 - Comparison Between Experimental Test Results And Theoretical Analysis For Joist Specimen

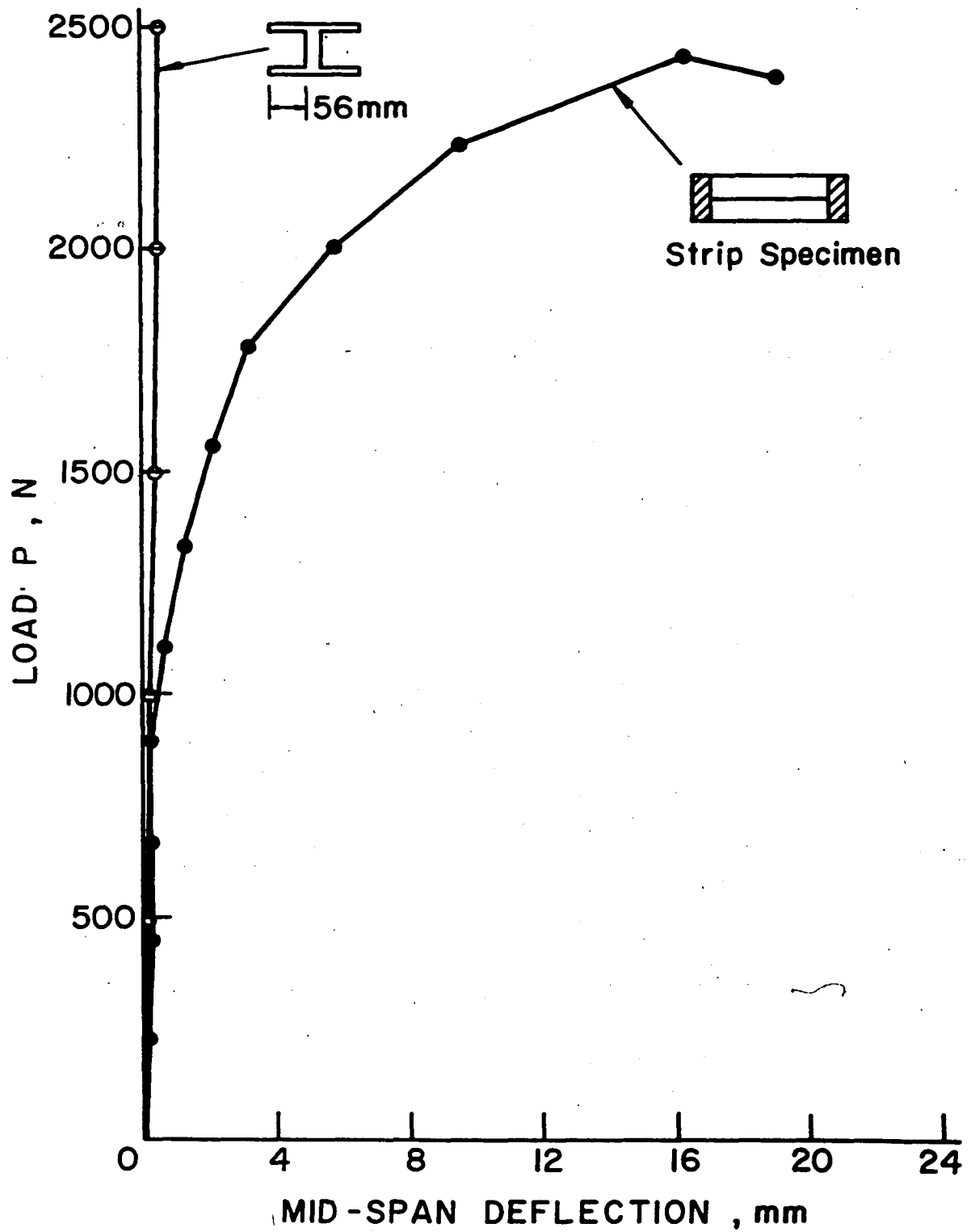
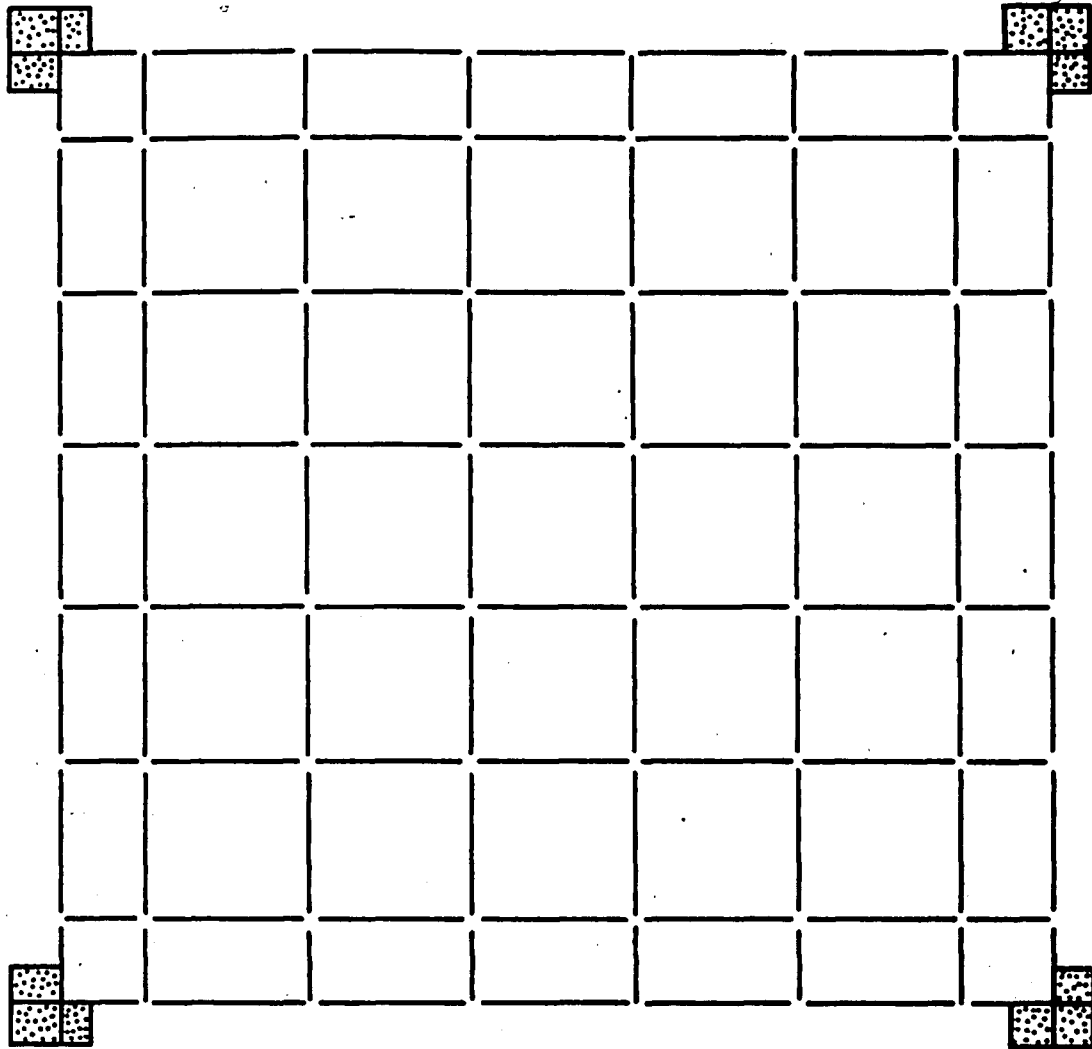


FIG. 36 - Comparison Between Experimental Results Of Strip Specimen And A Fictitious I-Beam With Flange Width Of 56 mm



— Beam Element  
▣ Plate Element

FIG. 37 - Discretization Of Finite Element Model

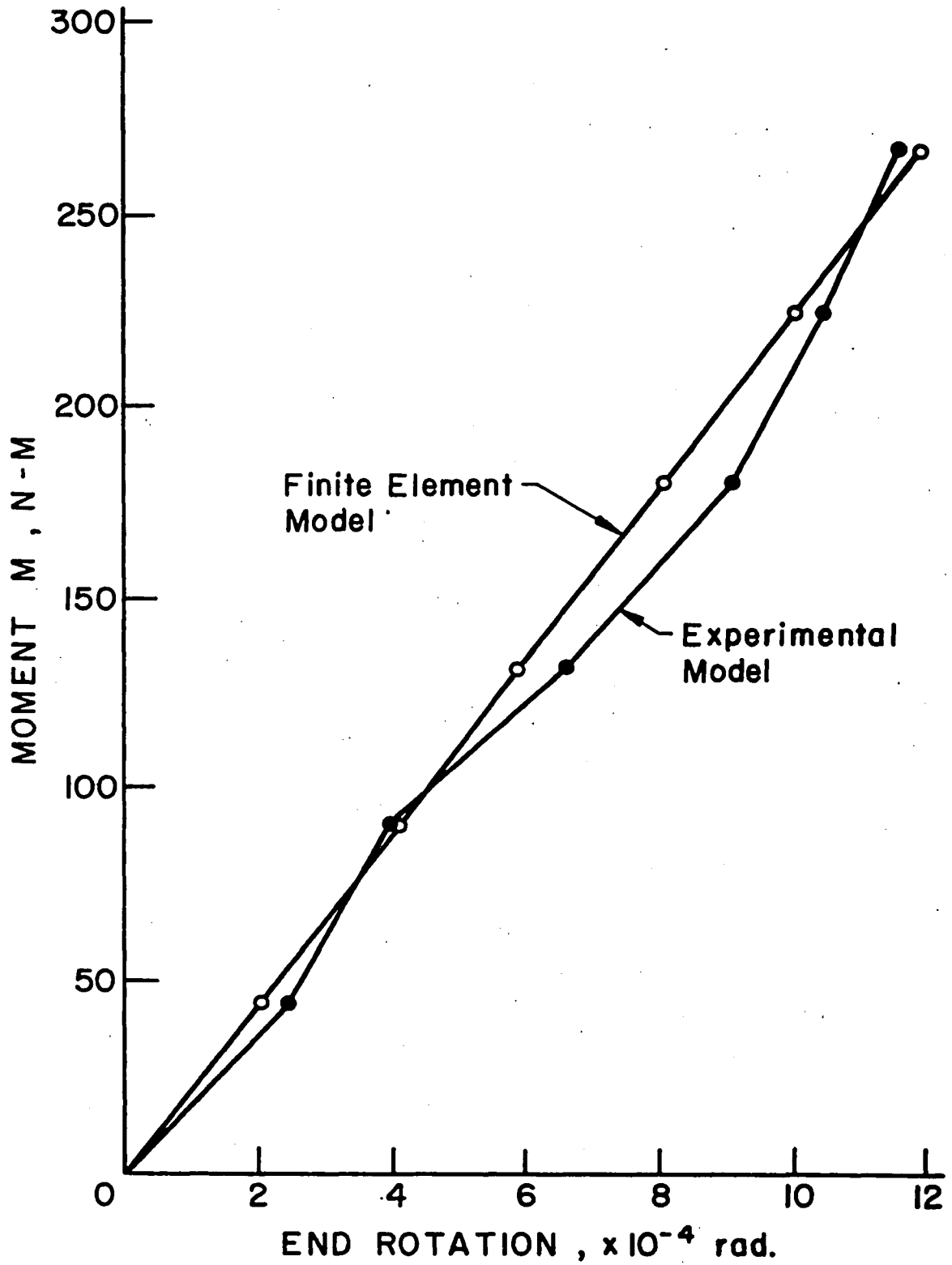


FIG. 38 - Comparison Between Experimental Results Of Slab Model And Finite Element Analysis For Test 4.



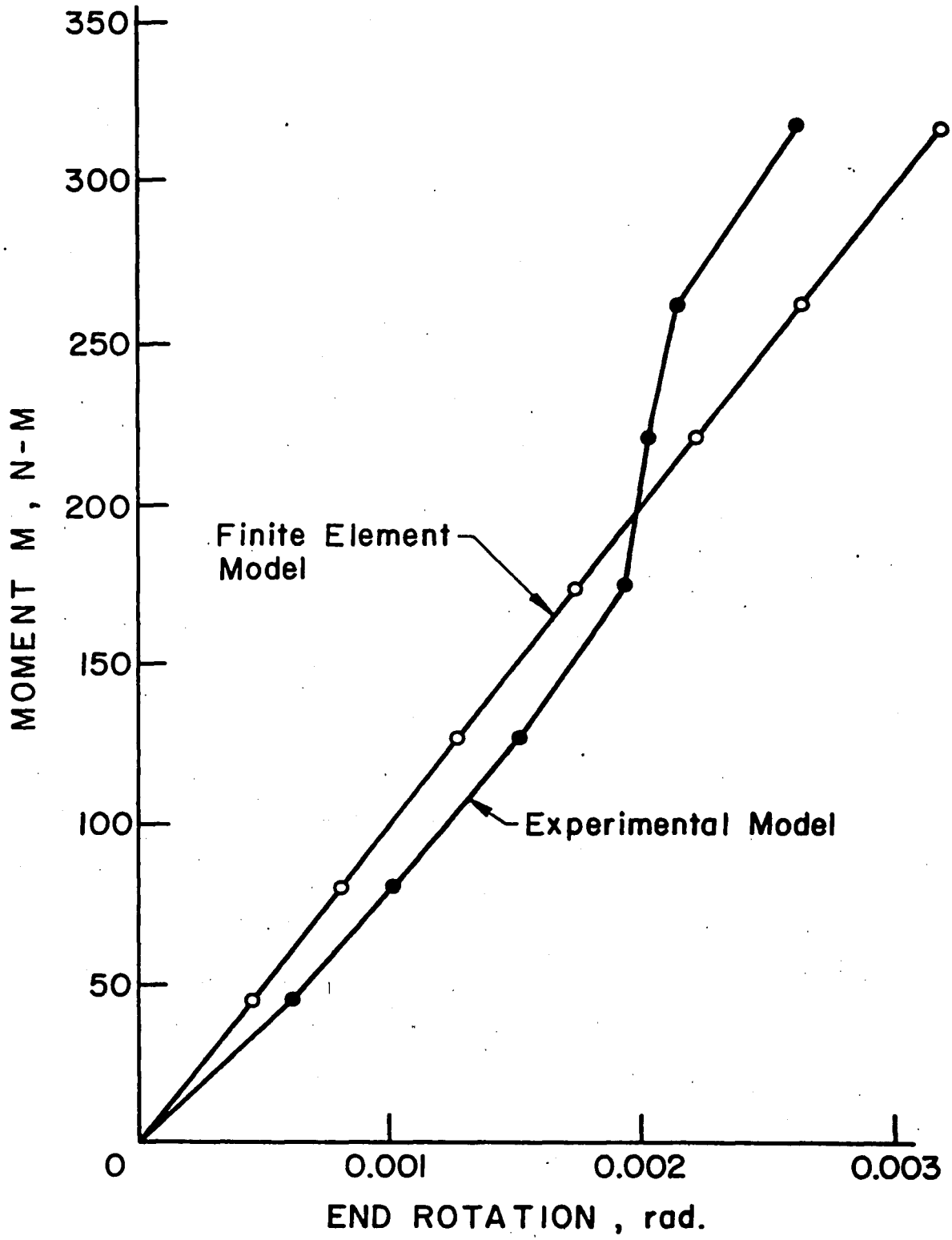


FIG. 39 - Comparison Between Test Results And Finite Element Analysis For Test 1

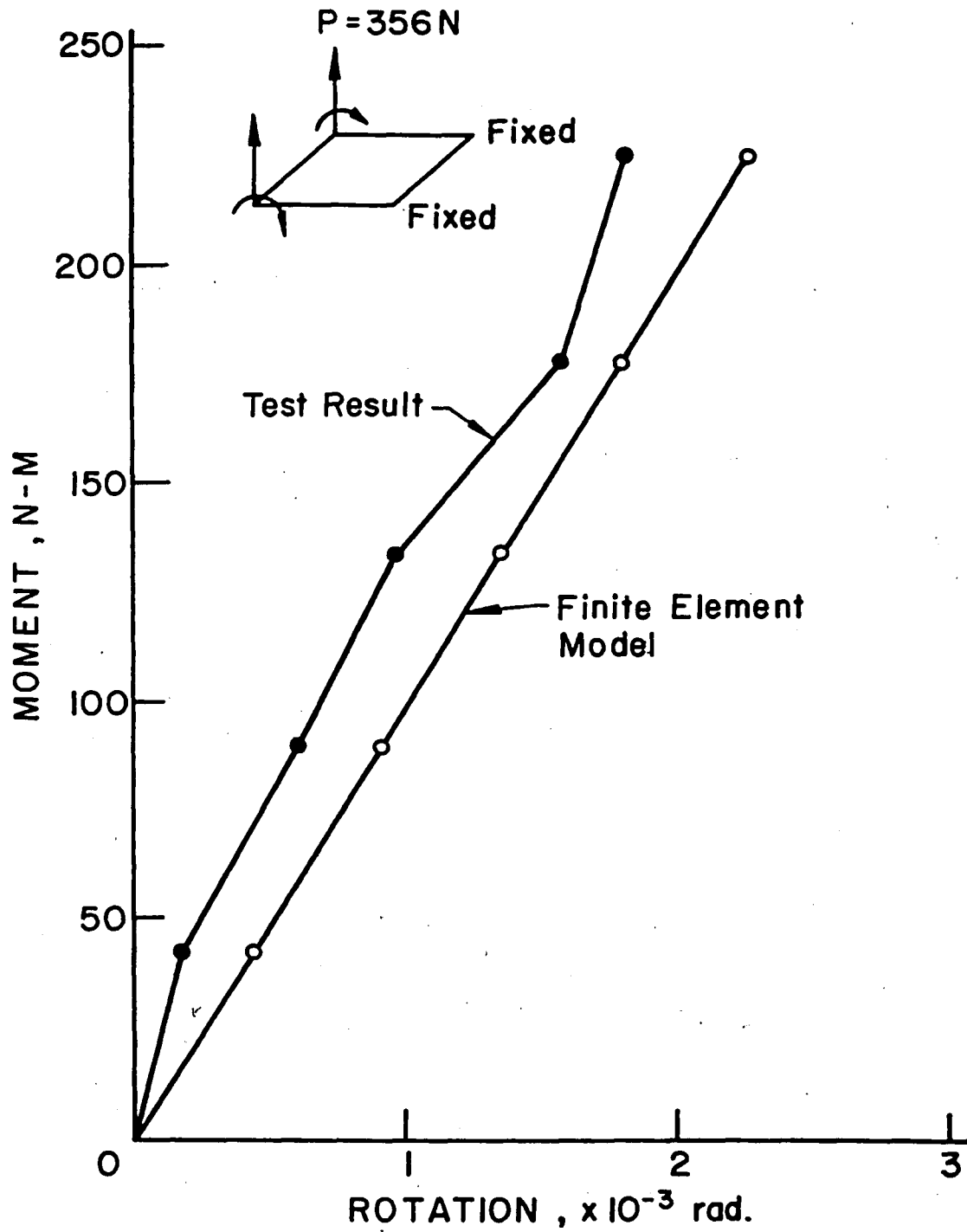


FIG. 4Q - Comparison Between Test Results And Finite Element Analysis For Test 2

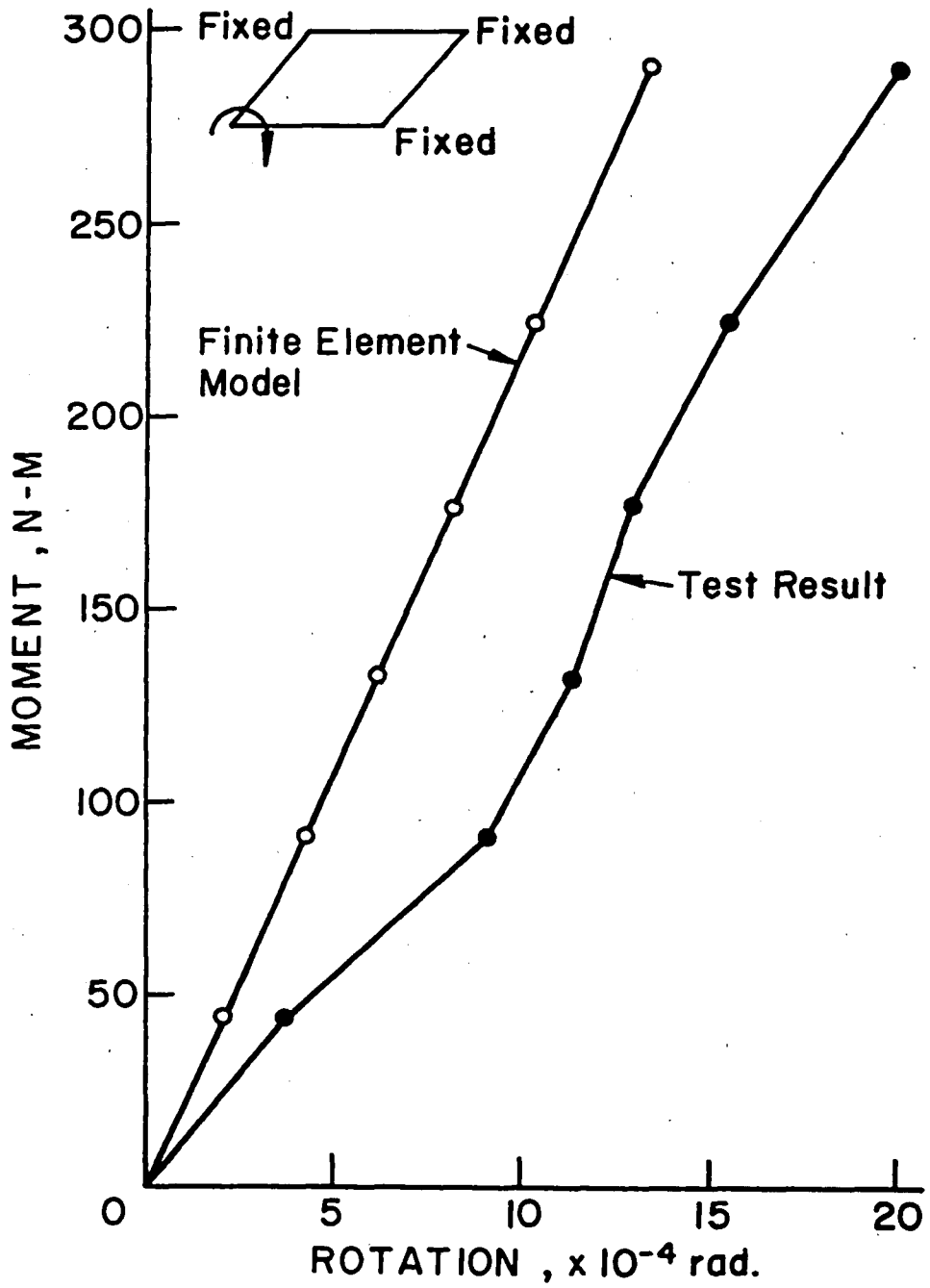


FIG. 41 - Comparison Between Test Results And Finite Element Analysis For Test 3

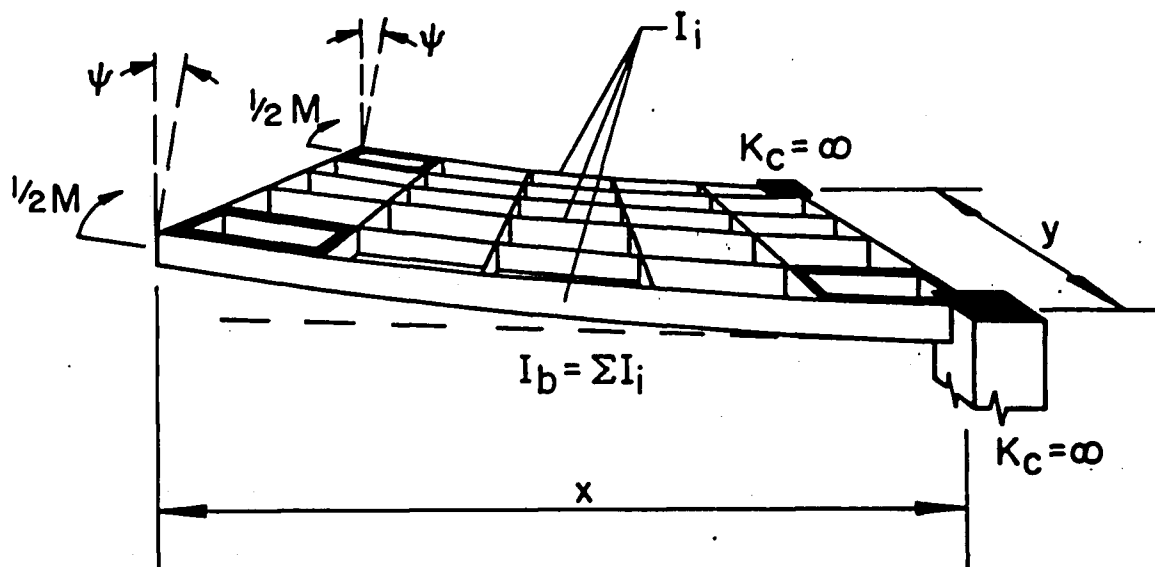


FIG. 42 - Parma's Model In Determining Coefficient Of Torsional Efficiency

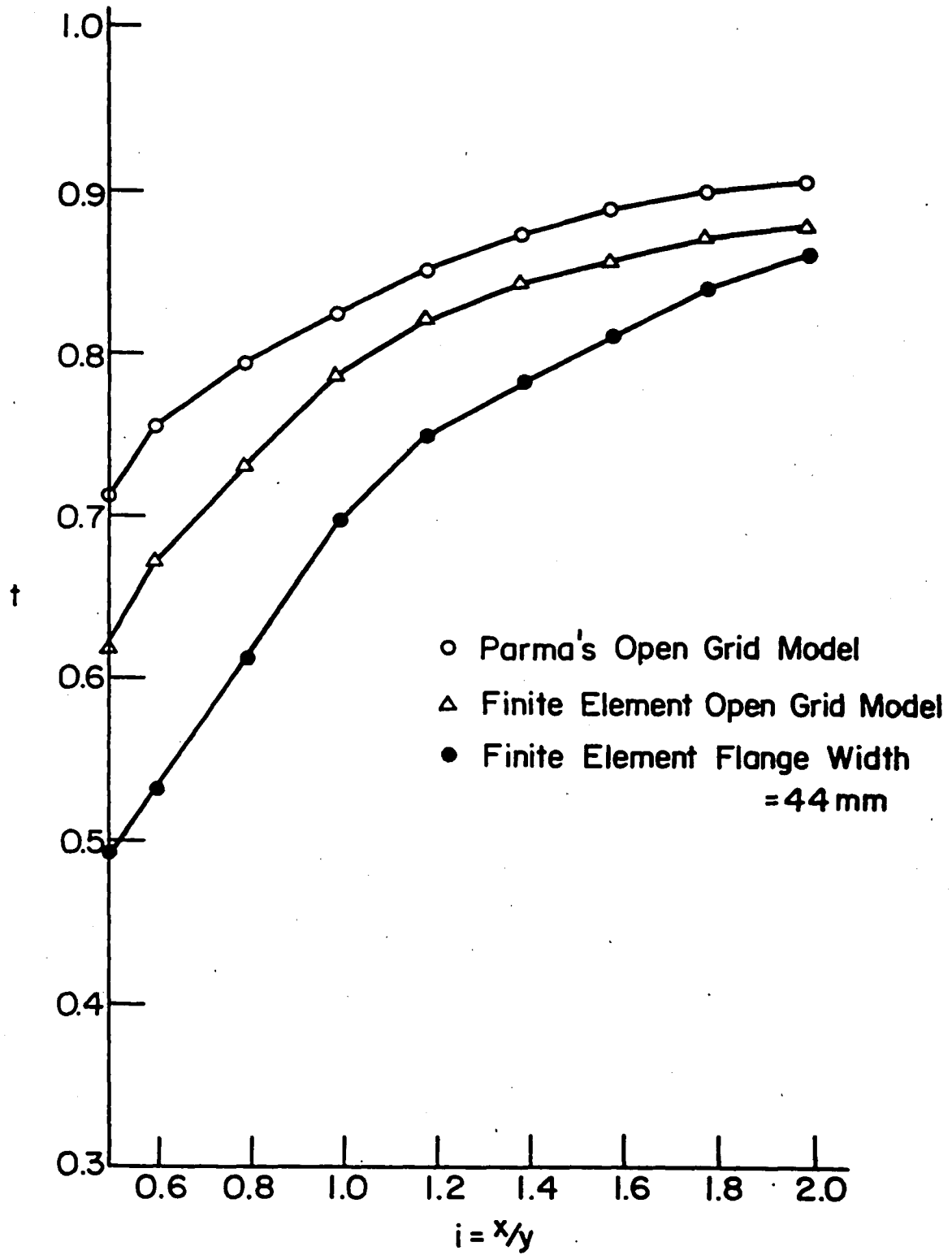


FIG. 43 - Torsional Coefficient Curves For Various Slab Models

## 8. REFERENCES

1. Parma, D. M., 1975  
ENTREPISO RETICULAR CELULADO, Independent, Bogota, Colombia.
2. Huang, T., Lu, L. W. and Palomino, A., 1977  
BEHAVIOR OF REINFORCED CONCRETE COLUMN-GRID STRUCTURES UNDER GRAVITY AND EARTHQUAKE LOADING, Unpublished research report, Lehigh University, Bethlehem, Pennsylvania.
3. Bathe, K. J., Wilson, L. E. and Peterson, F. E., 1974  
SAP IV - A STRUCTURAL ANALYSIS PROGRAM FOR STATIC AND DYNAMIC RESPONSE OF LINEAR SYSTEMS, University of California, Berkeley, California.
4. Gallagher, R. H., 1975  
FINITE ELEMENT ANALYSIS FUNDAMENTALS, Prentice-Hall, Inc., Englewood Cliffs, New Jersey.
5. Jofriet, J. C., 1973  
FLEXURAL CRACKING OF CONCRETE FLATE PLATES, ACI Journal, December, pp. 805 - 809.
6. Jofriet, J. C. and McNeice, G. M., 1971  
FINITE ELEMENT ANALYSIS OF REINFORCED CONCRETE SLABS, Journal of ST, A.S.C.E., ST3, pp. 785 - 806.
7. Winter, G. and Nilson, A. H., 1923  
DESIGN OF CONCRETE STRUCTURE, 8th Edition Revised, McGraw-Hill, New York.
8. Parma, D. M., 1970  
EQUIVALENT FRAME STIFFNESS SOLUTION FOR LATERAL AND GRAVITY LOADS, Paper presented at the Fall Convention of the American Concrete Institute, Mexico City, Mexico.
9. Scordelis, A. C., 1972  
FINITE ELEMENT ANALYSIS OF REINFORCED CONCRETE STRUCTURES, Proceedings of the Specialty Conference on Finite Element Method in Civil Engineering, Montreal, Canada, pp. 71 - 112.

## 9. VITA

Clarence Au-Young was born June 9, 1955, in Hong Kong, the son of Kwan and Sheung Au-Young. He was granted the Hong Kong School Certificate by New Method High School. In September 1973, he enrolled at Lehigh University where he received his Bachelor's Degree in the Department of Civil Engineering in June 1977. He continued his study at Lehigh University as a graduate student and research assistant in the Fritz Engineering Laboratory. He was associated with the research projects Dynamic and Static Tests of Beam from the Conneant Swamp Bridge, and Behavior of Reinforced Concrete Column - Grid Structures Under Gravity and Earthquake Loading.